Formation and Distribution of Porosity in Al-Si Welds

by

Pierre-Alexandre LEGAIT

A Thesis

Submitted to the Faculty

Of the

WORCESTER POLYTECHNIC INSTITUTE

In partial fulfillment of the requirements for the

Degree of Masters of Science

In

Material Science and Engineering

By

_____

May 2005

APPROVED:

_____

Diran Apelian, Howmet Professor of Mechanical Engineering, Advisor

_____

Richard D. Sisson Jr., George F. Fuller Professor of Mechanical Engineering

Material Science and Engineering, Program Head

ABSTRACT

Aluminum alloys are the subject of increasing interest (in the automotive industry, as well as aircraft industry), aiming to reduce the weight of components and also allowing a profit in term of energy saving. Concerning the assembly, riveting has been widely used in the aircraft industry, whereas welding seems to be promising in the car industry in the case of aluminum alloys.

Nevertheless, welding can generate defects, such as porosity or hot cracking, which could limit its development. One of the major problems associated with the welding of aluminum alloys is the formation of gas porosity. Aluminum alloy cleanliness remaining one of the aluminum industry's primary concerns, this project focuses on the formation and distribution of porosity in Al-Si welds.

A literature review has been performed, to identify the mechanisms of porosity formation in welds and castings. Porosity distribution in welds has been investigated, based on three different welding techniques: hybrid Laser/MIG welding process, the electron beam welding process, and the MIG dual wire welding process. Porosity distribution results provide information on to the porosity formation mechanisms involved during welding. A complete microstructure, microhardness and EDX analysis have been carried out, to describe and quantify the solidification process within the welds.

ACKNOWLEDGEMENTS

I would like to thank Pr. Diran Apelian, who was my supervisor at WPI. I would also like to thank Jader Furtado, my advisor at Air Liquide CRCD, and Michel Darrieulat, my advisor at the Ecole des Mines de Saint Etienne.

I would like to thank also M Richard Soula, the director of the CRCD for providing all facilities I need for my work in the Research Center, and to Pierre Bruchet, who was at the origin of the project with Prof. Diran Apelian (WPI) and Philippe Meyer (Montupet). During the transition period within the Metals Group with the departure of Pierre Bruchet to another position within AIR LIQUIDE, Savine Bockel-Macal and later Norbert Monier provided me with the environment and resources necessary to complete my work. I shall also mention Prof. Christophe Pijolat who was the correspondent at the Ecole des Mines de Saint-Etienne.

Also thanks to the engineers of the partner company, such as Philippe Meyer, Jean-Pierre Pielin, Pascal Poupardin, Thierry Rougé and Marie Fecourt, who provided samples of the aluminum parts to be welded and fruitful technical discussions on the formation of microporosity in the welds.

I won't forget the ones working at the CTAS and the CEPIA : Philippe Rouault, chairman of the CTAS, who allowed me to use the facilities for testing and analysing the welded samples; Michel Arnout, chairman of the CEPIA, who has trusted me during the all internship period; Corinne Chovet, responsible of the metallograhic laboratory, who welcomed me at the CTAS and helped me on my experimental investigations ; Jean-Marie Fortain, who spent time with me to give me directions and told me how to proceed; Christophe Herduin and Olivier Matile

from the CEPIA, who respectiveley informed me about the welding parameters used and gave advises to me; Christophe Schorr who was always available, very interested in my thesis, and who spent some time with me on the SEM; Nicolas Floros, who became my office colleague; my colleagues at the CTAS, I won't forget Xavier Chassang, Lyda Nutier, Christian, and the welders Christian, Christophe, Alain, Antoine.

TABLE OF CONTENTS

LIST OF FIGURES

Figures in Section 2

Figures in Section 3

LIST OF TABLES

Tables in Section 1

Tables in Section 3

SECTION 1: EXECUTIVE SUMMARY

Problem definition and thesis objectives

Aluminum alloys are the subject of an increasing interest by the car industry, as well as by the aircraft industry, aiming to reduce the weight of components and also allowing important energy savings in terms of fuel consumption.

Nevertheless, welding can generate defects, such as porosity or hot cracking, which could limit its development. One of the major problems associated with the welding of aluminum alloys is the formation of gas porosity. Aluminum alloy cleanliness remaining one of the aluminum industry's primary concern, this project actually concerns the formation and distribution of porosity in Al-Si welds, obtained by three welding techniques: a MIG dual wire welding process, a hybrid Laser/MIG welding process, and an electron beam welding process. A rolled sheet of aluminum alloy 5454 is welded to a cast part of aluminum alloy A356. The MIG technique provides a filler metal of aluminum alloy 4043.

Table 1: chemical composition of the aluminum alloys

Alloy	**Si (wt %)**	**Mg (wt %)**	**Mn (wt %)**	**Cu (wt %)**	**Ti (wt %)**
A356 (cast)	**7**	**0.3**	< 0.35	< 0.25	< 0.25
5454 (sheet)	< 0.25	**2.7**	**0.8**	< 0.1	< 0.1
4043 (filler wire)	**5.2**	< 0.05	< 0.05	< 0.3	< 0.2

The different problems to solve are

- To understand the mechanisms of porosity formation for each welding process,
- To investigate the chemical content inside the pores,

- And to understand the distribution of porosity and give tools introducing a future modeling work.

Methodology and approach

The thesis work has been directly and closely related to an industrial application. The goal was here to bring answers to the question of formation and distribution of porosity in Al-Si welds.

The first objective was thus to understand what is known about porosity formation in the scientific welding and casting literature. A literature review has been performed, aiming to identify the mechanisms of porosity formation.

A second objective was to examine the industrial welds, in order to characterize the distribution and the size of the pores inside the welds.

A third goal has been to analyze the solidification of the weld by different experimental methods, aiming to establish a relation between the porosity distribution and the solidification.

Concerning experimental methods, two main analysis have thus been carried out. The amount and the distribution of the porosity in welds has been identified by X-Radiography and optical microscopy, and the solidification has been evaluated inside welds cross sections by 3 different experimental methods : microstructure measurements and calculation of local solidification time have been carried out, whose results have been confirmed by micro-hardness measurements, and finally an evaluation of the composition gradients inside the welds has been performed by EDX (Energy Dispersive X-ray diffraction method).

After reaching these objectives, some mechanisms of porosity formation have been established thanks to experimental results and to the welding literature.

Presentation of key results

It is widely assumed in the literature that porosity is mainly due to hydrogen, very soluble in molten aluminum, which is rejected ahead of the solid/liquid interface during solidification, as it is the case in aluminum casting. Porosity will then form by nucleation and growth if the increasing hydrogen concentration reaches a threshold. Nevertheless, other porosity formation mechanisms which are more specific to a given welding technique could be involved as well. For instance, pores can be created by formation of a chemical gas during electron beam welding, or shielding gas can be entrapped due to the instability of the keyhole in high density welding processes. Porosity could be also due to evaporation of low boiling points elements.

Thanks to X-Radiography, we were able to detect pores whose diameter is greater than 300 microns, called macro-pores or macro-cavities, present only in the hybrid laser/MIG welds. In addition, optical microsopy provided informations on the micro-porosity content inside the welds.

Table 2 : Porosity content in welds

Porosity content (%)	**Welding techniques**		
	Electron beam	**MIG dual wire**	**Hybrid Laser/MIG**
Micro-Porosity content (%)	< 0.1	1.3	0.35
Macro-Porosity content (%)	0	0	3.32
Total porosity content (%)	**< 0.1**	**1.3**	**3.7**

Porosity distribution in welds has been investigated, concerning the three selected welding techniques. It appears clearly that microporosity in hybrid and MIG welds is mostly located close to the sheet, whereas macrocavities present in the hybrid welds are found to be close to the edges of the weld. It should be noticed that porosity distribution results provide information on the porosity formation mechanisms involved during welding.

A complementing microstructure study has been performed, aiming to understand more about the solidification, in terms of local solidification time and direction of solidification. The secondary dendrite arm spacing has been chosen as a microstructure index.

Table 3 : Dendrite arm spacing measurements and solidification time of the welds

Solidification parameters	**Welding techniques**		
	Electron beam	**MIG dual wire**	**Hybrid Laser/MIG**
Average dendrite arm spacing (in μm)	3.4	8.1	4.7
Average local solidification time (in seconds)	**0.025**	**0.93**	**0.13**

In terms of direction of solidification, it has been concluded that the welds have begun to solidify rapidly at the bottom and close to the cast, and it is thought that the last point to solidify would be located in the upper part close to the sheet.

Micro-hardness experiments confirm the results obtained through microstructure analysis by optical microscopy. Indeed, micro-hardness distribution results show the same type of solidification which has been described in the last paragraph.

Table 4 : Micro-hardness measurements in the welds

	Electron beam	**MIG dual wire**	**Hybrid Laser/MIG**
Micro-hardness (HV)	**102**	**84**	**98**

Finally, electron microprobe analysis has been carried out, hoping to eventually detect a gradient in composition due to segregation of elements during solidification of the welds. It appears that the silicon content has been homogenized in the weld bead due to the convection effect inside the molten metal during welding.

Unfortunately, it has been therefore difficult to establish a relation between the hardness and the silicon content

Based on the literature review and on the obtained results, mechanisms of porosity formation have been proposed for each welding technique under investigation. The mechanism of hydrogen segregation is proposed to explain the formation and the distribution of the micro-porosity in the MIG and hybrid laser/MIG welds.

Concerning the laser hybrid welding technique, the instability of the keyhole leading to shielding gas entrapment could be the main mechanism involved in the formation of macroporosity or macrocavities.

In the case of electron beam welding, it is thought that the pores are formed through a reaction between the molten aluminum and aluminum oxide present at the surface, forming Al2O gas.

In addition, it should not be excluded that porosity formation is partly due to the selective boiling of Magnesium present in the sheet. The MIG dual wire welds presents the coarser microstructure and the lowest hardness; we could thus believe that they solidified the less rapidly. The MIG welds also show almost two times less magnesium.

Table 5 : Magnesium content measurements in welds

	Electron beam	MIG dual wire	Hybrid Laser/MIG
Mg content (wt%)	**1.2**	**0.7**	**1.3**

This mechanism could be a cause of porosity formation, but this point needs to be confirmed by further electron microprobe analysis on porosity walls, by measuring the magnesium content in the pores.

Conclusion

Concerning every welding technique under investigation, the microporosity distribution analysis in welds seems to show that its formation is mainly due to hydrogen segregation during the alloy solidification, and the macroporosity formation is due to the instability of the keyhole in the case of the laser hybrid technique, as indicated in the literature.

Nevertheless, the contribution of other porosity formation mechanisms is not excluded; gas formation by chemical reaction, or evaporation of low boiling points elements such as magnesium could play a non-negligible role in the formation of porosity.

The electron beam welding technique optimized the level of porosity in Al-Si welds. Conversely, the greatest amount of porosity has been obtained by the hybrid laser/MIG welding. In between, the MIG dual wire welding technique presented suitable results in terms of porosity formation.

Nevertheless, it should be noticed that the relevance of these results is debatable since the welding by the three different techniques was not carried out under the same conditions of prior surface preparation.

SECTION 2: FORMATION AND DISTRIBUTION OF POROSITY IN ALUMINUM WELDS AND CASTS: A REVIEW

INTRODUCTION AND BACKGROUND

The two main types of porosity in aluminum casts are gas porosity, also called hydrogen porosity, and shrinkage porosity. For most metals, the transformation from the liquid to the solid state is accompanied by a decrease in volume. In aluminum alloys, the volumetric shrinkage that occurs during solidification ranges from 3.5 to 8.5%. Shrinkage occurs thus during solidification as a result of volumetric differences between liquid and solid states, and shrinkage porosity is generally more harmful to casting properties [1].

The following literature review will focus on the formation and the distribution of hydrogen porosity in welds and casts.

The purpose of this report was to determine from the available welding and casting literature how porosity forms during solidification of welds and casts. Different mechanisms of porosity formation, which can take place depending on the casting or welding process considered, will be presented.

POROSITY FORMATION AND DISTRIBUTION IN CASTING

Hydrogen and aluminum casting

Sources of hydrogen in aluminum casting

There are numerous sources of hydrogen in aluminum. Moisture in the atmosphere dissociates at the molten metal surface, offering a concentration of atomic hydrogen capable of diffusing into the melt [1]. Other sources of hydrogen contamination can include incompletely dried refractories, remelt ingot, master alloys, metallurgical metals, and other charge components, fluxes, tools, flux tubes, and ladles [1].

Degassing by the use of inert or active gases reduces hydrogen concentrations by diffusion into bubbles of the fluxing gas corresponding to the partial pressure of hydrogen in the fluxing gas. Spinning-rotor techniques have been developed that provide more intimate mixing, efficient gas-metal reactions, and shorter reaction times to achieve low hydrogen levels. The use of active fluxing gases and filtration removes oxides, permitting acceptable quality castings to be produced from metal with higher hydrogen contents.

Hydrogen solubility in aluminum

Hydrogen is the only gas with significant solubility in molten aluminum (see Figure 1). For pure aluminum, at the melting temperature 660°C, and 1 atmosphere of hydrogen gas, hydrogen solubility is in the range of 0.67-0.77 ml/100g in liquid and about 0.035 in solid. For liquid aluminum below 1000°C, the hydrogen solubility approximately doubles for every 100°C superheat [1].

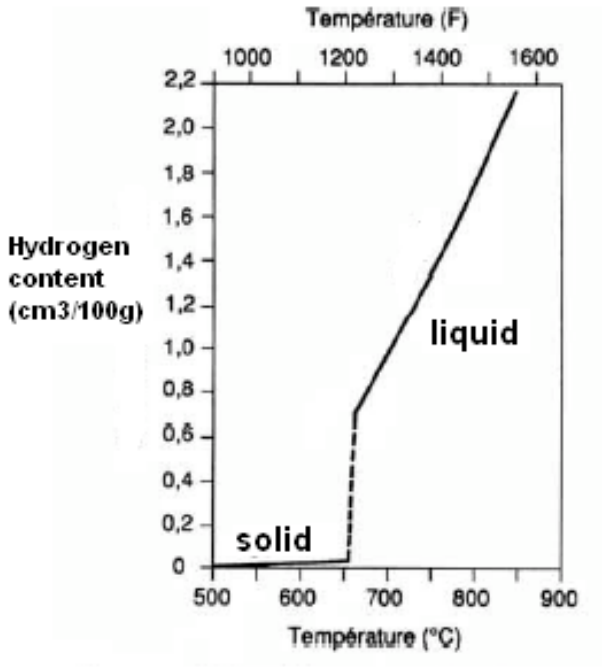

Figure 1: Hydrogen solubility in Aluminum [1]

It should be noted that alloy additions influence the hydrogen solubility in aluminum. A 6% magnesium addition almost doubles the hydrogen solubility [3], whereas Opie and Grant demonstrated that the solubility of hydrogen in aluminum decreased with increasing copper and silicon content [4].

Absorption of hydrogen

The barrier oxide of aluminum resists hydrogen solution, but disturbances of the melt surface that break the oxide barrier result in rapid hydrogen dissolution. Alloying elements, especially magnesium, may also affect hydrogen absorption by forming oxidation reaction products that offer reduced resistance to the diffusion of hydrogen into the melt and by altering liquid solubility.

Hydrogen atoms diffuse through the oxide layer and react with the melt. A typical hydrogen-producing reaction in the molten weld pool involving entrapped moisture is $2Al + 3H_2O \Rightarrow Al_2O_3 + 3H_2$.

According to Sievert's law,

$$[H] = K\sqrt{P_{H_2}}\ , \qquad (1)\ [3]$$

where [H] is the total volume of hydrogen in the liquid metal, K is a constant of proportionality, and PH2 is the partial pressure of hydrogen in the arc, expressed in atmospheres.

Hydrogen removal

Dissolved hydrogen levels can be reduced by a number of methods, the most important of which is fluxing with dry, chemically pure nitrogen, argon, chlorine, and freon. Compounds such as hexachloroethane are in common use; these compounds dissociate at molten metal temperatures to provide the generation of fluxing gas.

Gas fluxing reduces the dissolved hydrogen content of molten aluminum by partial pressure diffusion. The use of reactive gases such as chlorine improves the rate of degassing by altering the gas/metal interface to improve diffusion kinetics. Holding the melt undisturbed for long periods of time at or near the liquidus also reduces hydrogen content to a level no greater than that defined for the alloy as the temperature-dependent liquid solubility.

Nucleation and Growth of porosity

Since solubility is much lower in solid state than liquid state, hydrogen atoms then leave their position during solidification, and, by combining together, form hydrogen molecules, by rejection of the advancing solid/liquid interface. Porosity could also come from the nucleation of bubbles ahead of this interface, bubbles becoming frozen in the melt [3]. It seems that this process is controlled by nucleation and growth [6].

In more details, during solidification, and since most of the hydrogen is rejected at the solid-liquid interface, the interdendritic liquid becomes gradually enriched with hydrogen as the fraction of solid metal increases (see step I in Figure 2**Error! Reference source not found.**). Thus, as solidification progresses, the hydrogen content in the liquid increases, and eventually it exceeds its solubility limit. Ideally, a pore should nucleate at this point. However, the creation of a new pore requires the establishment of a new surface. Because of this surface barrier, the hydrogen concentration in the liquid continues to increase above the solubility limit until it reaches a value at which pores can form (step II in Figure 2**Error! Reference source not found.**). At that point, pores begin to nucleate, predominantly at the root of dendrites or at heterogeneous sites, such as inclusions. Then the small bubble (diameter < 20 microns) grows and hence the hydrogen content of the liquids drops rapidly (part III and IV in Figure 2)[1]. Pores could also coalesce with each other.

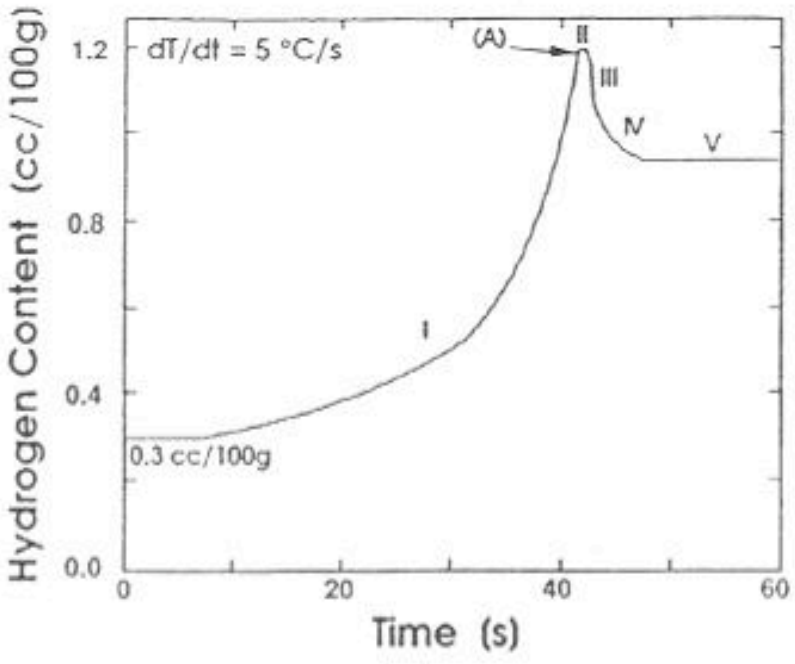

Figure 2: Evolution of hydrogen content before and after nucleation of the pores [7]

Thus the hydrogen solubility of an alloy system is indicative of the amount of hydrogen that can supersaturate the weld without forming pores. Alloy systems that have low solubility also have low hydrogen concentration threshold values of porosity formation and thus form porosity more easily [8].

The hydrogen concentration at which pores begin to nucleate depends on cooling rate rather than on the initial hydrogen content of the melt. The cooling rate has also a strong influence on the pore size and the density of pores.

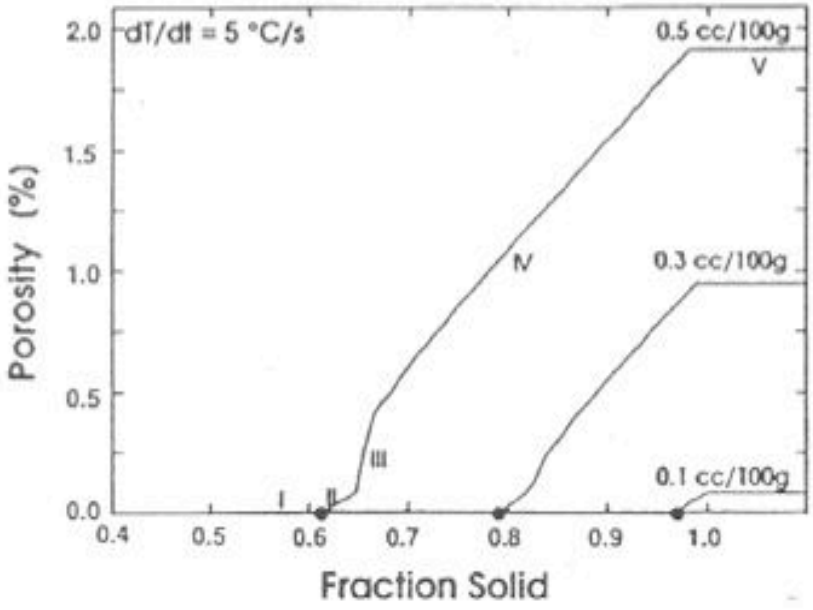

Figure 3: Increase of porosity level with the fraction solid [7]

The solid fraction at the beginning of pore nucleation is called the threshold solid fraction. Porosity does not form when the hydrogen content in aluminum alloys is lower than this threshold level (see Figure 3). The threshold level varies for different aluminum alloys due to their difference in hydrogen solubility. Greater amounts of hydrogen may be tolerated at higher cooling rates, because of smaller DAS that makes pore formation more difficult.

In addition, supersaturated hydrogen in the solid can diffuse into existing pores, causing pores to grow or new pores to form especially during heat treatment [1].

With increasing fraction of solid, the dissolved hydrogen in the liquid and solid at the liquid-solid interface both increase, and, as they do, the partial pressure of gas PH2 that would be in equilibrium with these dissolved gas contents also increases. According to Flemmings [9], a pore will form if:

$$P_{H_2} > P_g = P_0 + \rho_L g_r h + \frac{2\sigma_{gL}}{r} \qquad (2)$$

where P_{H_2} is the hydrogen gas pressure, P_g is the threshold pressure needed to form a pore, P_0 is the ambient pressure of the air, $\rho_L g_r h$ is the riser hydrostatic pressure, σ_{gL} is the surface energy of the pore, and r is the radius of the pore.

This hydrogen segregation phenomenon, followed by the nucleation and growth of pores, has been highlighted especially in the case of casting. Nevertheless, the welding process involves other mechanisms of porosity formation.

McDonald et al. [10] showed that very little porosity develops in the early stages of solidification during the casting of an Al-Si based alloy (AA601). The amount of porosity increases further when solidification is complete, and the critical time for porosity formation is during the last stages of solidification where there is a low fraction of liquid remaining, meaning after the formation of dendrites. In more details, the nucleation of porosity corresponds to the solidification of the intermetallics remaining (Mg2Si, Al8Mg3FeSi).

Shape of the pores

There are three types of pores. The macropores due to shrinkage, the micropores created at the roots of dendrites [1], called interdentritic shrinkage, and the gas pores [11]. The principal ways to measure this porosity are the density

measurements based on Archimede's principle and now X-Ray radiography, computer based image analysis pore by pore and tomography [12].

The interdentritic pores are smaller and close to each other, forming a group of pores called "cluster", whereas gas pores are bigger, not so close to each other and present a more circular 3 dimensional geometry (more regular in shape). It has been found that the average pore size of the shrinkage pore clusters is larger than the average size of the gas pores, thus the gas pores have a smaller "area of influence" but have always a larger pore density [11] (Al-7%Si casting).

But it should be noted that these clusters may not be due purely to interdendritic shrinkage, but to a combined effect of shrinkage and gas evolution, what has been proposed many times in the literature, even if the proof of its existence has been difficult to obtain [1] [11]. Then there is no evidence that pure shrinkage porosity occurs if the hydrogen level is above the threshold.

Nogi et al. [13] differentiate two types of pores, blowholes and wormholes. Blowholes are round shaped pores formed in the liquid phase and wormholes are narrow and long pores at the solid liquid interface. By welding an Al-Mg 5083 alloy both on microgravity and terrestrial environment, it has been found that blowholes grow by combining with other blowholes whereas wormholes do not combine with other wormholes or blowholes. Gravity does not affect any combination of bubbles, but affects the movement of bubbles larger than 135 μm.

When pores form at low fraction of solid, they are large and nearly spherical; at higher fractions of solid, they are more angular (on the size scale of the dendrite arms) and take the shape of the interdendritic spaces. This is why it becomes difficult to distinguish between gas- and shrinkage-caused voids when pores form at high fractions solid.

Parameters influencing the final porosity content

The weld porosity level is controlled by the initial hydrogen content of the material, the rate of hydrogen absorption, the solubility and the rate of hydrogen escaping [3]. Thermal parameters and weld metal composition have an influence on the hydrogen threshold of porosity formation, and have therefore an influence on the percentage of porosity, on the largest pore size, on the maximum pore area and on the porosity density [11].

Influence of the weld metal composition

Weld metal composition was found to be of primary importance in determining both the rate of hydrogen absorption and the hydrogen solubility.

As it is written in the last paragraphs, pure aluminum is prone to porosity formation. Nevertheless, Al-Mg alloys are much less likely to develop weld porosity [3], because the evaporation of magnesium can be considered as a degassing factor.

Concerning Al-Zn alloys, the tendency to porosity formation depends on the amount of alloying element. Indeed, it has been shown that Al-1%Zn are slightly more prone to porosity formation than pure aluminum whereas Al-6, 5%Zn alloys are significantly less prone to porosity formation than pure aluminum [3].

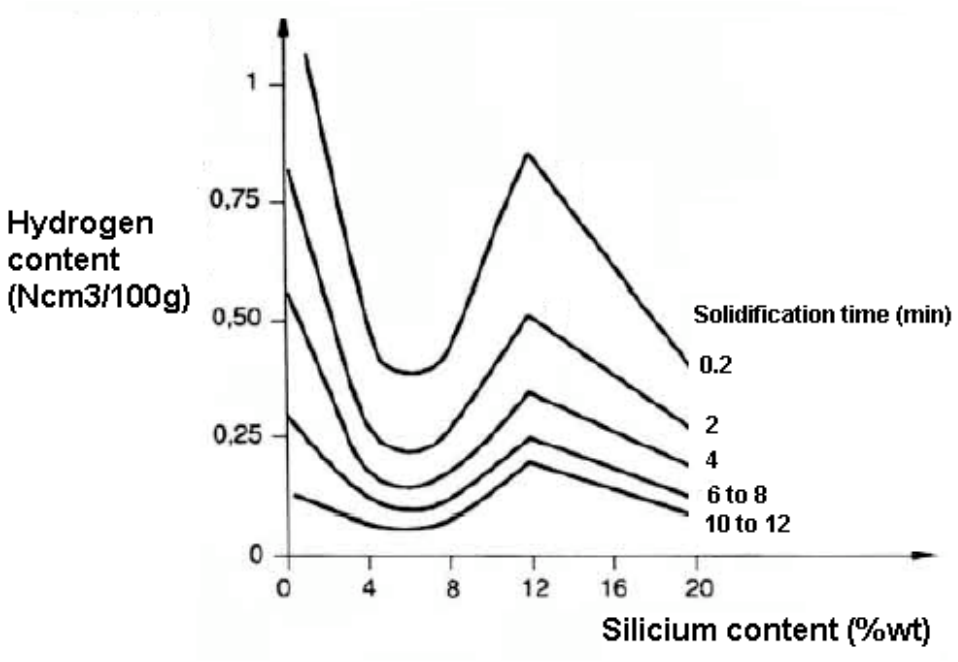

Figure 4: Influence of Silicon content on hydrogen solubility [6]

In fact, the solubility depends on the composition [6]. As examples, the addition of alloying elements such as Si, Cu, Mn, Ni decrease the solubility whereas the addition of Mg, Ti, or Zr will tend to increase it [6] (see Figure 4).

Influence of the thermal parameters

The level of porosity in casts depends not only on the weld metal composition, but also on thermal parameters, such as the solidus velocity, the local cooling time and the ΔT of solidification, the cooling rate, the temperature gradient, or the maximal temperature which has been reached during welding [1]. As an example, the amount of porosity increases with the ΔT of solidification and decreases with the cooling rate [6]. Thus, greater amounts of hydrogen may be tolerated at higher cooling rates [1].

In addition, the threshold value of hydrogen concentration is also dependent on pressure and on the number (n) and tortuosity (t) of liquid paths that exist in a solidifying dendritic network. The higher the product of these factors, the higher the hydrogen threshold.

Moreover, the level of porosity can also be varied after welding by heat treatment. For instance, a T6 heat treatment reduces the amount of porosity for an A356 alloy because the solute hydrogen can diffuse out under high temperature and long time [14].

Porosity distribution in casting

As previously mentioned, hydrogen is rejected ahead of the solid-liquid interface during solidification, because hydrogen is much more soluble in liquid aluminum than in solid aluminum. For this reason, as solidification progresses, the percentage porosity increases according to Figure 3.

Thus, porosity in casts will be concentrated in the last solidified parts of the cast. It is then admitted that the porosity distribution in cast depends on the shape of the mould, the temperature of each point of the mould and the direction of solidification.

This has been verified by S.T. McClain et al [15], who demonstrated by image analyses that as the thickness of the cast increases the porosity increases.

WELDING TECHNIQUES AND THEIR INFLUENCE ON POROSITY

Introduction on aluminum welding

Presentation of welding

The American Welding Society (AWS) definition for a welding process is "a materials joining process which produces coalescence of materials by heating them to suitable temperatures with or without the application of pressure or by the application of pressure alone and with or without the use of filler material" [15].

Welding employs pinpointed, localized heat input. Most welding involves ferrous-based metals such as steel and stainless steel. Nevertheless, even if aluminum is the most difficult alloy to weld because of its high thermal conductivity, aluminum welding seems to be promising because it presents a low density of 2.7 kg/dm3.

More information on welding and the different welding processes is reported in the appendix.

General welding parameters influencing the formation of porosity

The size, shape, distribution and amount of hydrogen pores generated in the weld are dependant upon the solidification mode, cooling rate, degree of convective fluid flow, welding parameters, bead shape, shielding gas mixture and external pressure [15].

Welding parameters have an influence on the thermal parameters involved in casting, parameters which have been mentioned in the last paragraph.

The welding parameters such as the welding current and the power density, the arc length, the welding speed, the flow rate and the composition of the shielding gas,

have an effect on the width and the depth of the fusion zone, and have therefore an effect on the hydrogen absorption and thus on the final level of porosity.

The weld bead shape is perhaps the most significant variables controlling the amount of porosity in welds. Welds that are narrow and have a high crown tend to trap porosity since individual pores must raise a long distance before escaping to the surface. And at the opposite, Woods [5] has shown that hydrogen porosity increases with increasing current in TIG welding, because it thus increases the volume of molten metal and the hydrogen absorption rate. Consequently, welding position controls the degree of porosity in the weld by means of the weld bead shape, which affects the bubble-escape distance and the direction of bubble buoyancy, and the escape of bubbles depends upon the molten weld pool geometry.

It was also found [25] that welds deposited in a helium atmosphere showed a much lower degree of porosity than those formed in argon or in a 65%He + 35%Ar mixturegas shield.

Moreover, other parameters, which are more specific to a given welding technique, can affect as well the percentage of porosity in welds. These specific parameters will be presented for each process under evaluation in the next paragraphs.

Hydrogen sources in welding

It is usually assumed that the basic reason for porosity formation is the presence of hydrogen. The sources of hydrogen most commonly encountered in commercial welding are hydrocarbons (grease, oils) and moisture contaminants on surfaces of the filler metal and plate [17]. Moisture can also be present in the drains and the bottle of gas, or on the welding tube. The shielding gas could thus contain hydrogen or water vapor.

Hydrogen can also be contained within the filler metal and parent metal [15]. Hydrogen atoms diffuse through the oxide layer and react with the melt, according to Sievert's law (see equation 1).

All aluminum surfaces involved in the welding process are to some degree contaminated, and three classes of contaminants may be present [17]:

- Surface compounds directly formed on aluminum surfaces as a result of chemical reaction between the atmosphere and the metal surface
- Substances physically or chemically adsorbed to the oxide layer, such as water, oil, greases, or solvents. This class of contaminants exhibits the highest weld defect potential.
- A surface layer of stressed, distorted metal that provides a deep layer for surface compounds of form by various oxidation reactions.

In the case of the MIG welding process, hydrogen in the filler metal has the highest influence on porosity[17].

Surface preparation

As an example, hydrogen content on the metals surface represents 70 to 80% of the total hydrogen content for both acetone degreased A356 and A5083 alloys [17].

It thus results from this a relatively heavy panel of operating conditions of preparation of the assemblies and respect of welding parameters, which strongly influence the final result. Examples are:

- Surface cleaning by degreasing, polishing, sand blasting or laser cleaning.
- Storage and use of the filler in tight, inerted and heated reels
- Position of welding and welding speed supporting degassing

Concerning the laser welding of A356, Pastor et al. [18] showed by SIMS analysis that previous surface preparation allows the removal of the oxide layer and allows a

significant reduction of the hydroxyl groups at the surface. Sand blasting provides good results in terms of porosity reduction, as polishing with 220 and 800 grade SiC provides even better results. Nevertheless, it appears that the final lowest level of porosity has been obtained through pulsed YAG laser cleaning.

Kudryashov et al. [19] showed that chemical treatments could provide good efficiency in terms of surface cleaning; the best results were obtained by pickling in a solution of NaOH alkali and scraping. However, according to Kudryashov, the most efficient method of treatment prior to welding is MAT (Magneto-Abrasive treatment). This method allows the reduction of the volume of hydrogen absorbed by the surface. Nevertheless, the type of surface cleaning has specific efficiency depending on the alloys. Haboudou showed that an A356 alloy has its surface hydrogen level three times higher than a 5083 alloy [12].

Storage time after cleaning and prior to welding also affects the porosity level in the weld pool, because the oxide film on aluminum alloys thickens with increasing exposure time [17].

MIG dual wire welding process

Presentation of the MIG dual wire welding process

Introduction on the single wire MIG process

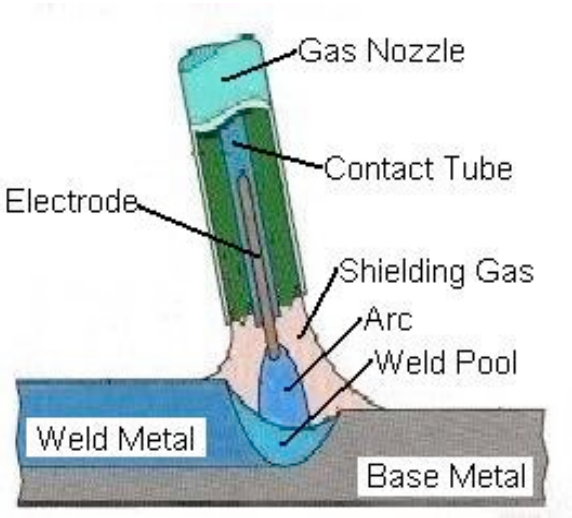

Figure 5: The MIG welding process [22]

Gas Metal Arc Welding (GMAW) is frequently referred to as MIG welding. The MIG process uses a continuous solid wire or tubular electrode to provide filler metal, and both use gas to shield the arc and weld metal. The electrode is solid, and all of the shielding gas is supplied by an external source, as shown in Figure 5. The shielding gas used has a dual purpose of protecting the arc ad weld zones from air and providing desired arc characteristics. A variety of gases are used depending on the reactivity of the metal and the design of the joint to be welded [21]. MIG welding is a commonly used high deposition rate welding process. Wire is continuously fed into the weld pool. MIG welding is therefore referred to as a semiautomatic welding process.

<u>Benefits of the MIG welding process:</u>

- All position capability
- Higher deposition rates than SMAW (shielded metal arc welding)
- Less operator skill required
- Long welds can be made without starts and stops
- Minimal post weld cleaning is required

The MIG welding technique requires the presence of a shielding gas. The shielding gas, forms the arc plasma, stabilizes the arc on the metal being welded, shields the arc and molten weld pool, and allows smooth transfer of metal from the weld wire to the molten weld pool. There are three primary metal transfer modes: spray transfer is most widely used, although globular transfer or short-circuiting transfer can be envisaged as well [21]. Transfer modes will be presented in more details in the next paragraph.

The primary shielding gasses used are pure Argon or a mixture of Argon combined with Helium.

CO2 is also used in its pure form in some MIG welding processes. However, in some applications the presence of CO2 in the shielding gas may adversely affect the mechanical properties of the weld [22].

The specific MIG dual wire welding process

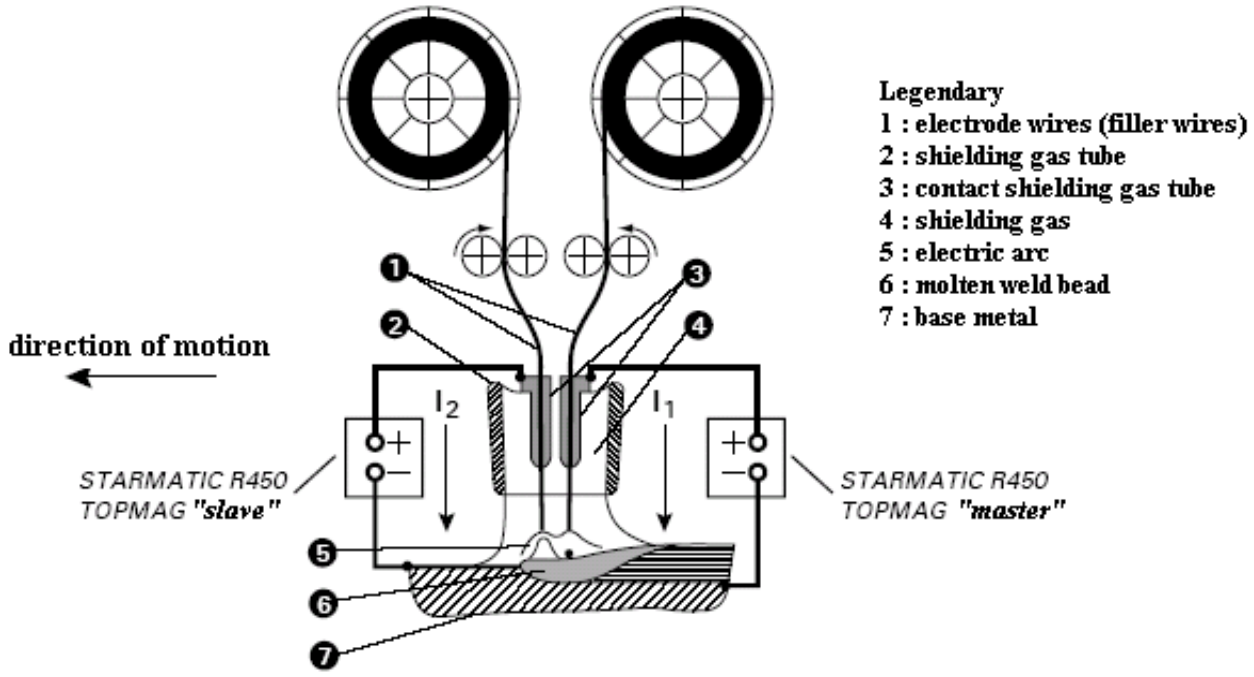

Figure 6: MIG dual wire welding process used (TOPMIG machine) [23]

The MIG dual wire welding, used industrially in many fields, is a process combining a good productivity with a great flexibility in use. In spite of its evolutions, welding speed increased only little up to now whereas the productivity remains a major concern [23].

The MIG dual wire welds were carried out with the TOPMAG machine at the Air Liquide Welding Research Center (CTAS). A schematic of the welding TOPMAG machine is represented on the Figure 6.

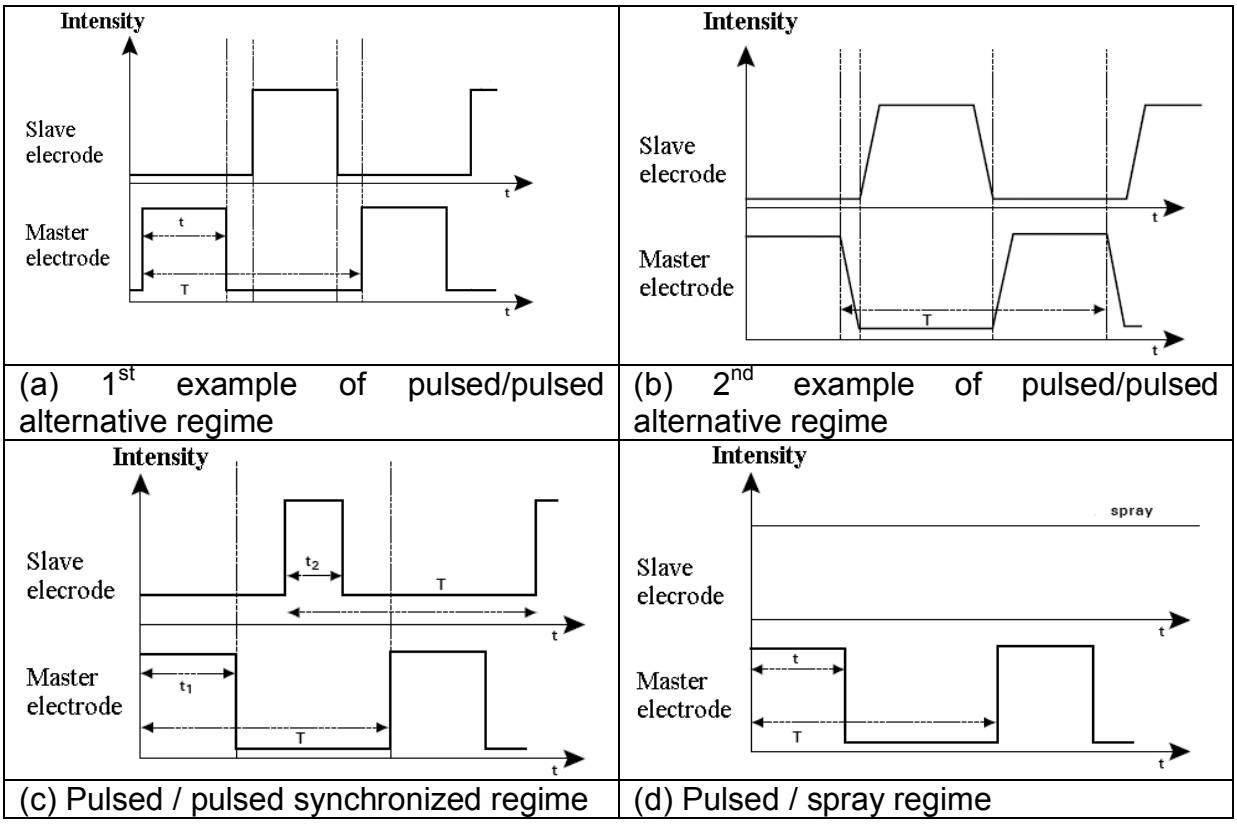

(a) 1st example of pulsed/pulsed alternative regime

(b) 2nd example of pulsed/pulsed alternative regime

(c) Pulsed / pulsed synchronized regime

(d) Pulsed / spray regime

Figure 7: Examples of intensity regimes used [23]

This technique consists in maintaining in the same torch the stability of two arcs of welding very close one to the other, each one of them depends on a specific power source. The intensity and frequency of each electrode can be varied. Some examples of variation are represented in the Figure 7.

Spray and globular transfer require relatively high welding currents while the short-circuiting transfer commonly uses low average currents. Shielding gases rich in Argon are required in the case of spray transfer for MIG welding [21].

The “spray” mode of transfer describes an axial transfer of small discrete droplets of metal at rates of several hundred per second. Argon of argon-rich gas mixtures are necessary to shield the arc. Direct current electrode positive powers are almost always used, and the amperage must be above a critical value related to the electrode diameter. The metal transfer is very stable, directional, and essentially spatter free [21].

If intermittent, high amplitude pulses of welding current are superimposed on a low level steady current that maintains the arc; the average current can be reduced appreciably while producing a metal spray transfer during the high amplitude pulses. Argon-rich gases are essential to achieve spray transfer. Pulsed arc operation is produced by the utilization of a programmed power source. Relatively large electrode diameters can be employed thin as well as thick sections of many base metals in all positions [21].

Porosity in MIG welds

Specific welding parameters influencing the porosity formation in MIG welds

The MIG dual wire welds are obtained by fixing the chemical composition of the filler wire, its speed, as well as the arc length and the mode of transfer. In addition, Binger et al. [24] showed that a welding frequency below 50 Hz minimizes the final porosity content. The filler wire metal composition can have an influence on the porosity formation, as it is added to the weld. It should be noticed that Binger et al. [24] developed a filler wire containing a certain level of cobalt, which reduces the size of

pores in the weld. Studies have shown that this reduction in size is due to the increase of the nucleation sites number. In addition, it has been found that for a squeeze cast A356 alloy, using Al-5Mg metal filler reduces the amount of porosity more than with an Al-5Si filler [14], showing that the amount of porosity depends on the filler wire composition.

Distribution of porosity in MIG welds

Gas porosity gathers always in an annular shape in the weld pool by cycles of convection or stream flow. The convection is due to buoyancy force (but apparently negligible), electromagnetic force, and surface tension gradient on the weld pool surface [14]. If the convection has an upward sweeping action, gas bubbles can escape, if it has a downward sweeping action, gas bubbles can be caught by solidification. A small surface tension gradient and a great electromagnetic force usually develops a convection pattern from the center downward to the bottom of the pool and then there can be a movement upward along the fusion boundary [14].

The gas pores are usually distributed at the top of the weld pool because if some pores are entrapped, they are always distributed at the top layer of the fusion zone [14].

Bubbles “banding zones” can also be observed in aluminum welds. The bubble enriched or depleted zones form by exactly the same principle, as do solute banding lines in welds. In solidification theory, a sudden increase in solidification rate at the solid-liquid interface will result in a solute-rich band of solidified metal but also a porosity-entrapped zone. Conversely, a sudden increase in the growth rate of the interface causes solute and bubble depletion. Such banding zones are observed in aluminum welds due to the characteristic periodicity or fluctuation in solidification rate that is inherent in welding [17].

Specific ways to limit porosity formation in MIG welds

A method to reduce the level of porosity is to increase the convection movements of the weld bead [26] [17]. Thus, during solidification, the flow of the molten metal will break dendrites forming, and prevents porosity to form in the inter-dendritic spaces. Convection accelerates the nucleation, growth and ultimate escape of bubbles from the molten weld pool [17]. Different methods are known to vibrate the molten bead during welding:

- Mechanical vibration of the base metals
- Application of external electromagnetic fields
- Application of important variations of welding current

In the case of the MIG welding, another solution is to choose filler wire metal that would increase the number of nucleation sites. Indeed, it has been shown by Binger et al. [24] that the addition of cobalt in the filler wire leads to a reduction of the porosity size. But this doesn't lead to the reduction of porosity level, and for this reason this method has not been commercialized.

Hydrogen contaminants adsorbed on the surface of the welding wires influence formation of porosity to a much higher degree than the presence of the same impurities in the parent metal. This is due to the involvement, in the process of weld deposition, of a large percentage of the wire surface – as compared to the volume – and also of the filler material[25]. For this reason, cleaning the filler wire would lead to the reduction of porosity.

Wheatley [27] imagined that air could be entrained through the filler wire conduit during MIG aluminum welding. Indeed, it is probable that a zone of reduced pressure exists at the point where filler wire exits the contact tube. It is therefore possible that sufficient air could be sucked into the arc atmosphere to raise moisture content

enough to cause an increase in weld porosity. For this reason, the design of welding heads should be such that air cannot pass from the body of the head to the arc atmosphere via the contact tube.

Shinoda and Matsumoto [28] showed that in the case of non-alloyed aluminum welding, porosity content could be decreased by the addition of SiCl4 in shielding gas.

Laser Hybrid welding process

Presentation of the laser hybrid welding process

Introduction on the laser welding technique

Similar to the electron beam, a focused high-power coherent monochromatic light beam used in laser beam welding (LBW) causes the metal at the point of focus to vaporize, producing a deep penetration column of vapor extending into the base metal (keyhole). The vapor column is surrounded by a liquid pool, which is moved along the joint producing welds with depth to width ratios greater than 8:1. Yttrium aluminum garnet (YAG) lasers may be used for spot welding thin materials, joining microelectronic components, and other tasks requiring precise control of energy input to the workpiece [27].

Advantages of the laser beam [27]:

- A vacuum environment is not required for the workpiece because the laser beam is easily transmitted through air. However, reactive workpieces must be protected from the atmosphere by inert gas shields
- X-Rays are not generated by the beam
- The laser beam may be readily shaped, directed, and focused with reflective optics, thereby allowing easy automation

- The tendency for spiking and root bead porosity is lee than with Electron beam welding

The specific laser hybrid welding process

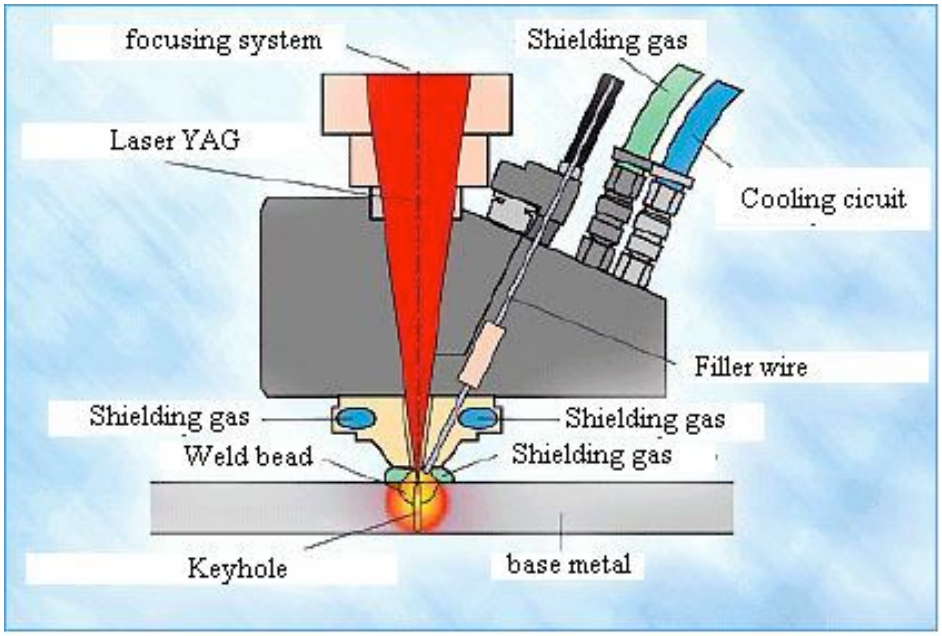

Figure 8: Principal of the laser hybrid welding technique [30]

The hybrid welding process consists in combining an arc welding process (MIG, MAG, TIG or plasma) with a laser welding process (Nd:YAG [Yttrium Aluminum garnet] or CO2). In our case, a MIG torch combined with a laser YAG composes the hybrid welding process (Figure 8).

This welding technique presents an economic advantage compared to the laser welding process, as well as technical advantage compared to laser welding and MIG welding in terms of welding speed and process tolerances [30].

The laser welding technique is currently widely used in the industry. This technique allows narrow and deep weld beads at high welding speeds, and because of its high density of energy, the laser process generates low level of residual stresses. This process requires a high investment, a precise preparation before welding, and can with some alloys lead to hot cracking.

The MIG welding presents opposed characteristics: A low economic investment, a greater tolerance considering the preparation before welding, but a limited welding speed and depth of the weld. It also generates important level of residual stresses.

Thus the hybrid process combines the advantages of the laser process to the advantages of the MIG process.

Main advantages of hybrid welding process in comparison with LASER:

- Improvement of welding speed
- Enlargement of squeezing sheets tolerance
- Enlargement of joint tracking tolerance

Applications:

- Sheet joining (steels and aluminum) in automotive body-building
- Continuous high speed welding of stainless steels tubes
- Pipe welding
- Large thickness welding

Porosity in hybrid Laser/MIG welds

Welding parameters influencing the porosity formation

Concerning the laser beam welding, the type of beam (single or dual beam) [12] and the type of laser (CO2 or Nd:YAG) have an impact on the thermal parameters. In addition, the focal lens length and the distance to the weld are also important parameters to consider because the keyhole would become unstable if the beam is a little defocused. Indeed, porosity formation can be due to the instability of the keyhole (see page 14).

Distribution of porosity

Micropores whose diameter is lower than 300 microns, and macropores and cavities whose diameter is greater than 300 microns can be found in laser beam welds. An important part of the porosity rate in welds is due to the presence cavities. Micropores are due to dissolved hydrogen in the weld bead, whereas cavities are formed by keyhole instability [12].

Pastor et al. [15] showed by x-ray radiography analysis that cavities had formed due to the instability of the keyhole are localized mostly at the edges and at the root of the bead.

Ways to limit porosity formation

In the case of the hybrid Laser/TIG welding of a Magnesium alloy, Liu et al. [31] obtained experimental results which showed that lacking of shielding gas for laser beam is the dominant cause of porosity formation, and hydrogen is not the main cause to form large pores. Nevertheless, a favorable weld without porosity can be obtained by appending lateral shielding gas for laser beam (see Figure 9). When the laser shielding gas is coaxial, it strongly disturbs the arc stability.

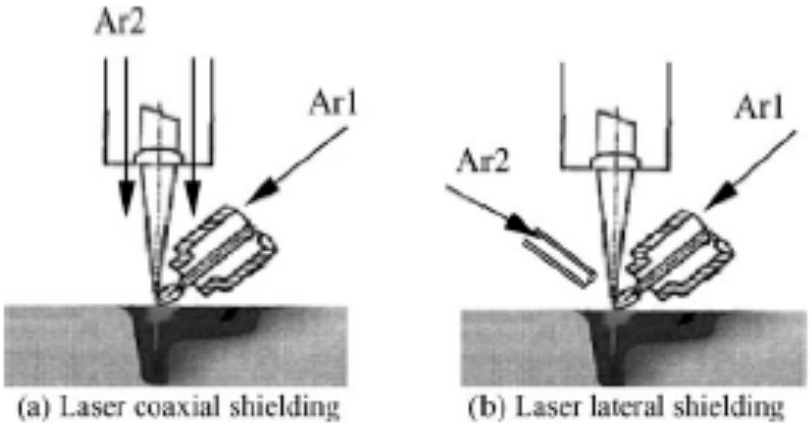

Figure 9: Shielding by coaxial laser versus lateral laser [31]

Concerning laser beam welding, a surface preparation using a pulsed YAG laser reduces the hydrogen sources responsible for microporosity generation, and

well-known surface preparation method. Nevertheless, it has been shown that other techniques such as sand blasting or SiC paper polishing lead to a greater reduction of porosity rate [12].

Haboudou et al. [12] carried out another investigation. They inserted an optical prism between the collimating lens and the focusing lens of the laser, in order to divide the beam into 2 spots. Through this experiment, they showed that, compared to single spot welding, the dual spot welding stabilizes weld pools and keyhole dynamics, and reduces the porosity rate.

An other way to reduce porosity consists in stabilizing the keyhole. To proceed, one should make sure that the defocusing and the welding speed are set in the optimum conditions (see page 14).

Electron beam welding process

Presentation of the process

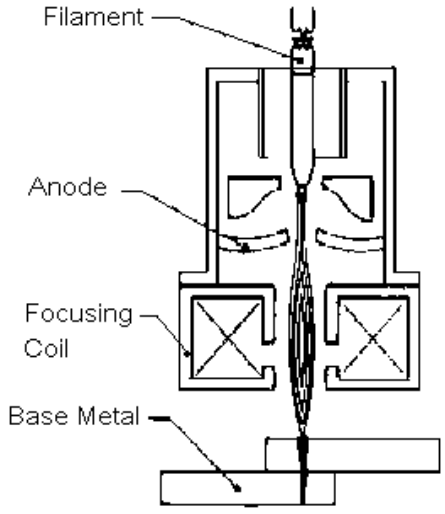

Figure 10: Principal of the electron beam welding technique [22]

Electron Beam Welding (EBW) (Figure 10) is a fusion joining process that produces a weld by impinging a beam of high-energy electrons to heat the weld joint. Electrons

are elementary atomic particles characterized by a negative charge and an extremely small mass. Raising electrons to a high-energy state by accelerating them to roughly 30 to 70 percent of the speed of light provides the energy to heat the weld [22]. The concentrated beam of high-velocity electrons produces intense local heating. Each electron penetrates its own short distance and gives up its kinetic energy in the form of heat. With high beam energy, a hole, also called a keyhole, can be melted through the material [31]. The generation of the keyhole is explained in more details in a next paragraph.

An EBW gun functions similarly to a television picture tube. The major difference is that a television picture tube continuously scans the surface of a luminescent screen using a low intensity electron beam to produce a picture. An EBW gun uses a high intensity electron beam, rated at from 30 kV to 175 kV and 50 mA to 1000 mA [31], to target a weld joint. The weld joint converts the electron beam to the heat input required to make a fusion weld [22].

The electron beam is always generated in a high vacuum. The use of specially designed orifices separating a series of chambers at various levels of vacuum permits welding in medium and nonvacuum conditions. Although, high vacuum welding (up to 10^-6 torr [31]) will provide maximum purity and high depth to width ratio welds.

<u>Advantages of electron beam welding [22]</u>

- Single pass welding of thick joints
- Hermetic seals of components retaining a vacuum
- Low distortion
- Low contamination in vacuum
- Weld zone is deep, narrow and almost parallel-sided [31]

- Heat affected zone is narrow
- Dissimilar metal welds of some metals
- Uses no filler metal

The depth to width ratio of electron beam welds can be greater than 10:1 [31].

Limitations of electron beam welding:

- High equipment cost
- Work chamber size constraints
- Time delay when welding in vacuum
- High weld preparation costs
- X-rays produced during welding
- Rapid solidification rates can cause cracking in some materials

Porosity in electron beam welds

Welding parameters influencing the porosity formation

The accelerating voltage is a good example of specific parameter to the electron beam welding. In addition, the focal lens length and the distance to the weld, in other words the beam focus, which could lead to an unstable keyhole if the beam is not focused, as well as in the case of a laser beam welding. The process also involves two other basic variables: the welding speed and the beam current [31].

Distribution of porosity

Nogi et al. [13] also showed that concerning the welding of a Al-Cu alloy by electron beam, the pores are segregated only in the upper part of the bead for electron beam welding and are widely distributed in the upper half of the bead for TIG welding, this distribution being approximately constant with the welding speed. The distribution differs for both of these welding processes because for TIG the pores are formed

during cooling due to the decrease of hydrogen solubility and for electron beam welding the pores are formed during heating at the molten pool center where the temperature is the highest so there is more time for the bubbles to rise to the upper end. For TIG welding, the surroundings of the bubbles are solidified to some extent and the movement of bubbles is thus heavily restricted.

Under microgravity (10-5 G) there is no convection due to gravity (Buoyancy force). Then for TIG welding Nogi et al. [13] find more pores because they can't escape and for EB welding they find fewer pores because the small size of the bubbles is maintained due to the lack of coalescence and they disappear.

Ways to limit porosity formation

According to Fujii et al., the number of pores significantly decreases under microgravity (level of microgravity: 10-5 G) [33].

In addition, the number of pores increases as the thickness of the oxide film increases [33]. Therefore, the use of any method that would reduce or limit the oxide film would decrease the number of pores in the welds.

THEORY OF POROSITY FORMATION DURING SOLIDIFICATION OF WELDED COMPONENTS

Introduction

In 1983, though a great deal had been reported on the causes of porosity, little was known, little was known about the mechanism of pore formation relative to solidification mechanics, nucleation, growth and transport of gas bubbles in the weld pool. It was still uncertain whether nucleation of hydrogen bubbles occurs in the bulk liquid or along the solid-liquid interface [15].

This paragraph aims to present the different mechanisms of porosity formation reported in the welding literature before 2005. Some of the mechanisms, which will be mentioned in this section, are specific to a given welding technique, whereas some other mechanisms of porosity formation could be involved during welding by any technique.

Welding is a good example of process, which could easily generate porosity if its formation is not prevented.

Pores can be found in solidified aluminum alloys. Processes such as casting, as well as welding, are good examples of processes, which could easily generate porosity if its formation is not prevented. Fujii et al. [33] proposed 5 causes of porosity formation concerning the electron beam welding process:

- A decrease in solubility of dissolved elements in the molten pool during cooling and solidification, main mechanism involved during casting
- A chemical reaction,
- The keyhole phenomenon,

- The evaporation of the elements having a high vapor pressure,
- Trapped gas between the root faces,
- Physical trapping of the shielding gas.

The first mentioned mechanism, due to the solubility gap between the solid and the liquid state, is the main mechanism of porosity formation involved during casting.

These mechanisms mentioned above have a different influence on porosity formation for each welding technique. And some mechanisms could be specific of a known welding process.

First of all, it is to wonder what is the chemical content of the pores. Many publications assume that these gas pores contain hydrogen, aluminum and its alloys being very susceptible to hydrogen absorption [3]. But it is still possible to find other elements in the pores (alloying elements, Argon or Helium) [9], especially in the case of welding. Indeed, Pastor et al. believe that the main constituent of the macropores formed during laser welding is shielding gas [15]. The question of the gaseous chemical composition of the pores does not lead to an obvious answer, and it usually depends on the process as well as on the porosity formation mechanism.

We will now focus on the main porosity formation mechanisms involved in casting, MIG dual wire welding, hybrid laser/MIG welding and electron beam welding.

Porosity formation by hydrogen segregation

Hydrogen absorption

Hydrogen can be formed by the chemical reaction between aluminum and moisture according to the chemical reaction $2Al + 3H_2O \Rightarrow Al_2O_3 + 3H_2$. In MIG welding particularly, virtually all of the moisture, grease and other hydrocarbon contaminants on the wire surface are immediately vaporized in the arc and converted into atomic

hydrogen, which is then available for absorption into the molten pool. Nevertheless, in welding conditions, Lancaster [34] states that Sievert's law does not hold in aluminum weld metal because hydrogen gas is immediately converted to ionized hydrogen in the arc and subject to a strong electromagnetic field as it passes across the arc and enters the weld pool. Thermodynamically, the value of K in equation 2 does not adequately reflect the complex thermal and electromagnetic gradients involved in the welding process. Nevertheless, it has been reported by most investigators that the solubility of hydrogen in molten aluminum is still a function of the square root of the hydrogen pressure despite the fact that ionized hydrogen is entering the pool directly. Undoubtedly, the value of K (see equation 2) under welding conditions has increased. For this reason, extremely high hydrogen concentrations are possible in the molten pool of aluminum arc welds.

Nucleation and growth of porosity

Nucleation of bubbles

It is assumed that the mechanism of nucleation and growth of bubbles, involved in casting (page 2) can take place under high solidification rate during welding [17] [25]. Porosity will form if the equation (2) (Flemmings) is valid.

Porosity can nucleate either in the bulk liquid or along the solid-liquid interface [17]. In weld pools, there are ample nuclei for heterogeneous nucleation of bubble. The concept of heterogeneous nucleation of bubbles in aluminum alloys has been attributed to impurity inclusion concentrations. In high purity alloys having virtually no heterogeneous nuclei available, high levels of supersaturation of hydrogen are observed but very little porosity results. However, when aluminum alloys contain substantial quantity of oxides and other inclusion to act as nuclei, much less

supersaturation and greater porosity occurs during solidification. Nucleation sites in the bulk liquid could be elements such as aluminum oxide [17] or cobalt [34].

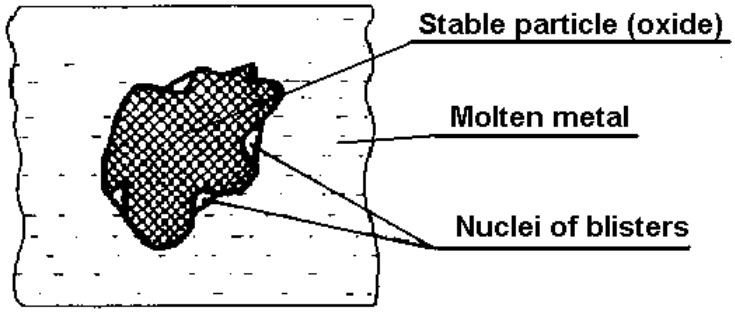

Figure 11: Mechanism of blister formation on oxides in the areas not wetted by the molten metal [25]

According to Mazur [25], the nuclei of porosity consist of microvoids located on the uneven surface of stable particle such as an oxide wetted by the molten metal (see Figure 11).

Thus, for porosity to be present in aluminum welds the hydrogen concentration should exceed locally 0.69 cm3/100g and microdiscontinuities should be present on the particles surface.

Growth of bubbles

Basically, the growth occurs by hydrogen diffusion into a preexisting stable pore or by coalescence with a neighboring pore. Thus, pore growth rate and size are expected to be dependent upon several factors, which are the cooling rate or solidification rate of the weld, the diffusion rate of hydrogen, the hydrogen concentration in the molten metal, and the concentration of stable nuclei. Consequently, rapid cooling rates retard growth by eliminating the time available for diffusion and coalescence, whereas slow cooling rates allow sufficient time for bubbles to escape.

In addition to diffusion of hydrogen into the bubble, bubble growth is greatly accelerated by coalescence. Coalescence of pores is a function of two primary

parameters, which are the time in the molten bead, and the velocity of the bubbles. According to Stoke's law, the upward velocity of a bubble is given by:

$$v = \frac{2}{9} g r^2 \frac{\rho_L - \rho_H}{\mu} \qquad (3)$$

where g is the acceleration of gravity, r is the radius of a bubble, and ρL and ρH are the densities of liquid aluminum and hydrogen, respectively. In a simple case where no convection is present, a large floating bubble will overtake a smaller one in its path and coalescence will occur. During welding, rapid convection produced by electromagnetic, thermal and limited surface tension driven fluid flows produces fluid velocities far greater than those predicted by Stokes' equation. Clearly, variations in the solidification rate, convection fluid flow and heat flow distribution within the molten pool will significantly influence the rising velocity as well as the coalescence capability of the pores in the molten pool.

This is confirmed by Saperstein's results[35], which found that fast cooling rates produce only a minimal volume of many fine pores while very slowly cooled welds contain very few but large pores. It is at the moderate levels of weld cooling rate of heat input that produce the maximum total volume of porosity that have a medium average pore size.

The interstices between cellular dendrites provide localized regions in which bubbles can grow, but detachment and flotation into the molten pool is less likely. If the dendrites fully solidify around a bubble while the bubble is still small, the resulting pore will tend to be spherical due to the high surface tension. Larger interdendritic bubbles will more easily become non-spherical or angular since the increase in bubble surface tension is less than the force of cellular-dendrites converging laterally. However, these larger bubbles have greater buoyancy and tend to detach and

a bubble detaches itself, it grows to sizes substantially larger than the primary dendrite arm spacing [17].

Shape of the pores

Chalmers [37] has shown that the relative rate of cellular growth compared to bubble growth is an important factor in determining the shape of pore. If the welding rate is fast and small intercellular bubbles cannot grow as fast as the advancing cells, isolated pores remain entrapped between adjacent cells. At very slow cooling rates, bubbles may grow at a rate greater than the advancing cells.

Thus, solidification morphology and kinetics not only determine where the available spaces will be for the nucleation and growth of bubbles, but also the size, shape and distribution of porosity in the solidified weld metal. Interdendritic pores, also called wormholes because they are elongated, are formed at medium cooling rate. Their elongation form is due to the inability for the bubble to detach itself from the intercellular space, the bubble still growing in a direction parallel to the cell axis. Finer porosity will form at higher cooling rate, whereas larger spherical pores will be able to form at lower cooling rate. Large spherical pores are usually indicative of nucleation at temperatures above the liquidus [17].

The mechanism of porosity formation due to hydrogen may be involved during any technique welding.

Porosity need not only form at the liquid state, but can form in the solid state, for example in the heat affected zone, or in the solidified weld zone during further cooling. This is referred to as secondary porosity. Secondary pores are usually 1-2 microns in diameter and can be located either in the weld or in the heat affected zone. However, in multipass welds, secondary pores can grow and coalesce to an x-ray detectable level.

Compositional effects

Certain aluminum alloys tend to result in higher concentration of porosity than others. Nevertheless, in terms of relative importance, the influence of alloy composition is second to that of the partial pressure of hydrogen in the arc atmosphere. In fact, the influence of alloy addition is due to the influence of alloy content on the solubility of hydrogen in aluminum. The alloy additions may also alter the solidification range and modify the solidification mode, which may further contribute either positively or negatively to the formation of porosity.

For example, increasing magnesium concentration increases the hydrogen threshold for porosity formation and consistently results in decreased porosity. Copper and silicon present an inverse effect [17].

Evaporation of alloying elements with a high vapor pressure

A second source of porosity for aluminum alloys containing magnesium might be linked to the low boiling temperature of magnesium in the case of arc welding. Indeed, the weld bead is heated by welding up to very high temperature. At this temperature, Aluminum is mostly molten, but some alloying elements can evaporate. Magnesium for instance is expected to evaporate during welding because of its low vaporization temperature (1090 °C at atmospheric pressure).

According to Haboudou et al. [12], an Al-Mg alloy is expected to generate much more porosity than the A356 alloy in the case of laser welding. But according to Woods et al [3], Al-Mg alloys are much less likely to develop weld porosity.

According to Pastor et al. [15], concerning the laser beam welding process, the reduction in magnesium concentration was more pronounced during conduction mode welding.

Porosity formation could be partly due to evaporation of alloying elements concerning any welding technique, if the boiling temperature is reached inside the weld bead.

It has been also shown that vaporization of magnesium in the weld pool causes also a difference in the precipitating mechanism (to Mg2Si) of aluminum alloys, resulting in the decrease of mechanical properties [15].

Laser beam welding: Keyhole phenomenon

It has been generally accepted for TIG and MIG welding of aluminum alloys that the hydrogen being highly soluble in liquid aluminum is the dominant cause of porosity in the welds. However, the mechanism of porosity formation in laser welds of aluminum alloys has not been cleared yet, because the behaviors of molten pool and keyhole during the rapid cooling are not clear.

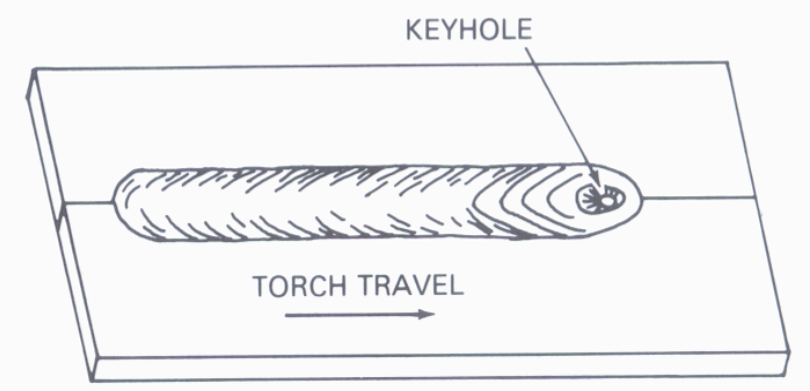

Figure 12: Pictorial representation of the keyhole [34]

Three possible considerations have been suggested to state the mechanisms of porosity formation in laser welds of aluminum alloys [38]. The porosity formation might be attributed to:

- dissolved hydrogen in the molten pool,

- formation of an unstable keyhole due to the evaporation of the alloying elements with low vapor pressure such as magnesium and zinc,
- and turbulent flow of the molten metal.

According to Papritan [39], the keyhole is a vapor column surrounded by a thin cylinder of molten metal (see Figure 12).

Keyhole Generation

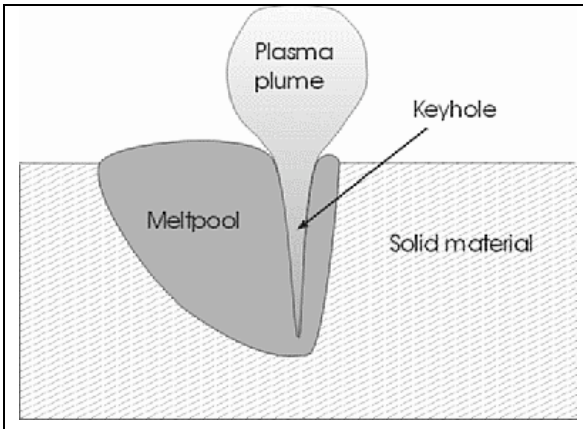

Figure 13: Keyhole welding [40]

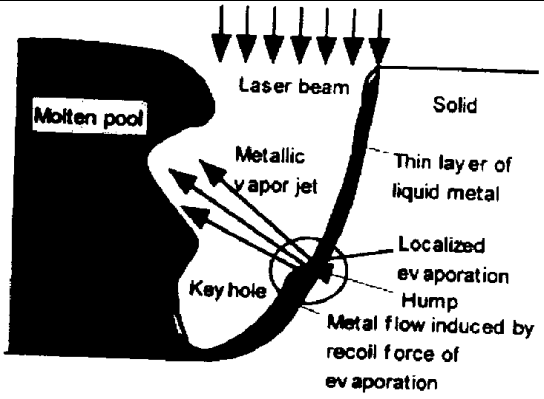

Figure 14: Metal flow induced by recoil force of evaporation [17]

Compared to the arc welding techniques, the laser beam can provide a density of very high energy, up to 106 W/cm2. Such a density of energy is too significant to be able to be evacuated by conduction. Thus, the target metal vaporizes locally creating a depression in the molten metal. While the beam is progressing during welding, the back of the keyhole solidifies [40] (Figure 13 and Figure 14).

Welds can be made without a keyhole, where melting takes place by conduction of heat from the surface, but welding speeds are lower.

Keyhole stability

Experimental results showed that the instability of the keyhole was the dominant cause of macroporosity formation during laser welding of thin plates of aluminum alloys. Hydrogen did not play a significant role in the porosity formation [15].

Matsunawa's research group [40] has found that evaporation of metal does not occur uniformly on the keyhole front wall but takes place locally, and thus the position of the evaporation site on the front wall changes with time.

Owing to the strong dynamic pressure exerted by the evaporated metal vapor jet, the rear wall of the keyhole fluctuates violently, and the metal jet ejected from the keyhole opening changes its direction and speed temporally.

These unstable keyhole phenomena promote the entrapment of shielding gas in the keyhole, resulting in the formation of characteristic macroporosity.

According to Pastor et al. [15], the stability of the keyhole can be greatly affected by the extent of defocusing of the laser beam. Thus, focusing the beam can lead to a considerable reduction of porosity (Figure 15).

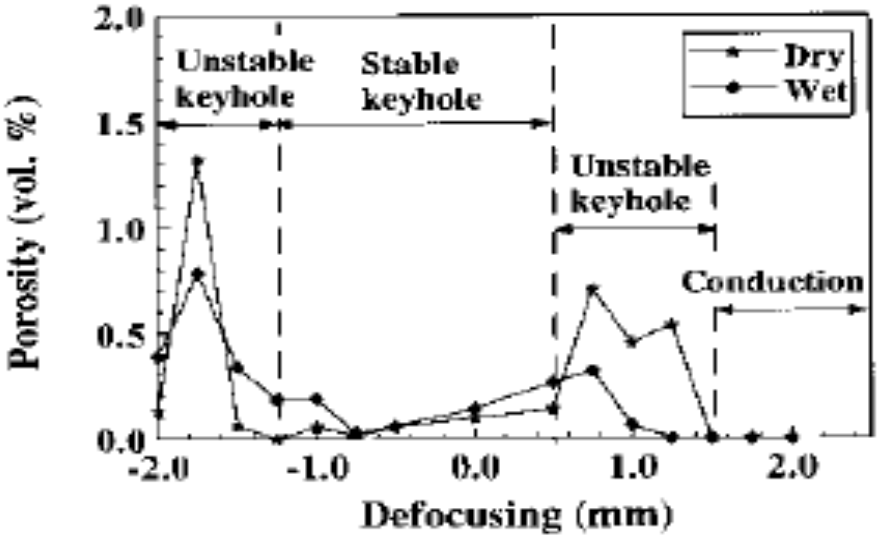

Figure 15: Porosity produced at several defocused values with dry and wet helium as the shielding gas- Alloy 5754. Nominal power 3kW, welding speed 150 inches/min, shielding gas flow rate 5.66 m^3/h of helium [18]

Pastor et al. showed that the welding speed has an influence on the stability of the keyhole (Figure 16).

Increasing the welding speed allows the keyhole to be unstable, knowing that the keyhole will disappear (conduction mode) if the welding speed becomes too

important. It should be noted that the porosity level is minimized as welding is performed in “conduction mode” conditions.

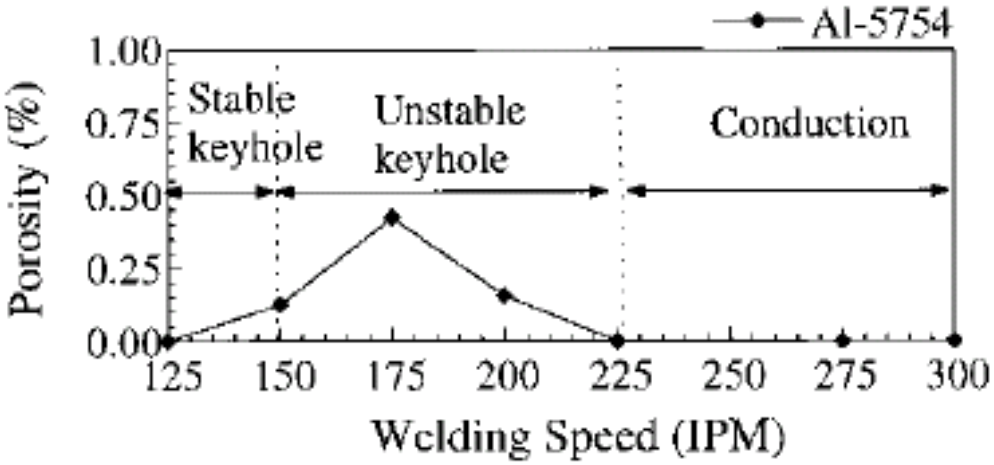

Figure 16: Influence of welding speed on pore formation during laser welding of aluminum alloy 5754 using a focused beam. Nominal power 3kW and shielding gas flow rate 5.66 m^3/h of helium [18]

Haboudou et al. [33] showed that evaporation of Magnesium during keyhole mode welding destabilizes the keyhole. Thus, an aluminium alloy welds containing aluminum will present more cavities than an aluminum alloy weld without magnesium. Indeed, Haboudou showed by EDS that Mg content on porosity walls is at least 1% greater than the initial Mg content in the base metal concerning laser welding of A5083 alloy. Important quantity of Silicium (10-20 wt%) has also been locally found on porosity walls, it is thus believed that its vaporization temperature (around 2500°C) has been reached inside the keyhole. In addition, the presence of oxygen confirms the entrapment of oxygen coming from the atmosphere via the keyhole [17].

According to Kutsuna [38], as laser welding speed increases, the number of pores with diameters less than 50 microns significantly decreases. Experimental results indicated that the behavior of porosity formation is closely related to the nucleation and growth of bubble formation during solidification of molten metal. Increasing

welding speed, i.e. solidification rate reduces the time allowed to the bubble to grow[38].

It seems that cavities with irregular shapes are mainly due to keyhole instability, whereas micropores with a more circular shape are due to hydrogen dissolved in molten metal.

Chemical content of the pores

Kutsuna [38] showed by gaseous chromatography that pores contain more than 80% of hydrogen in both keyhole mode and conduction mode welds. For A3003, A5052 and A6061 alloy welded in conduction mode (penetration less than 1.5 mm), the porosity gas in the welds contains about 90 vol% of hydrogen and the rest of nitrogen. Other types of gas have been detected depending on the welding mode and materials (see Figure 17). For A5083 and A5182 alloy welds with deeper penetration by keyhole type welding, the porosity gas is about 80 vol% of hydrogen, and helium as shielding gas was detected.

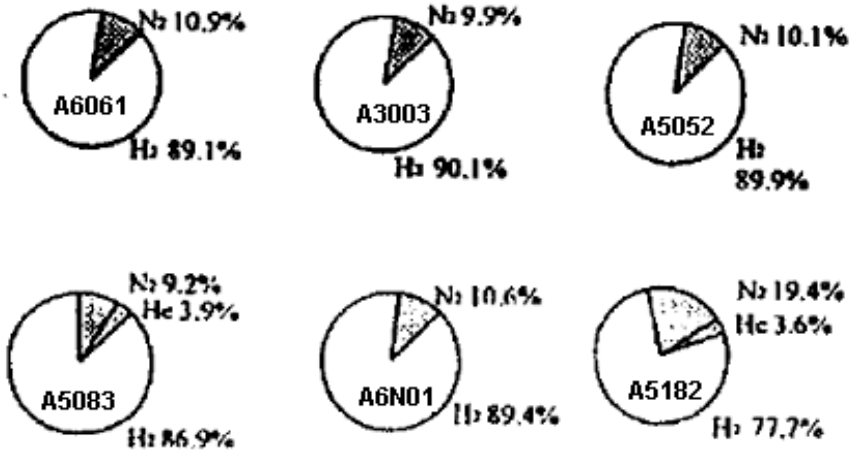

Figure 17: Chemical composition of gaseous content for different aluminum alloys (shielding gas He, 10l/min, laser CO_2, P=3kW, V=17mm/s) [38]

It is thus believed that helium, used as a shielding gas, penetrates trough the keyhole and can be entrapped in pores. These experimental results validate the keyhole instability mechanism of porosity formation.

Electron beam welding: Chemical reactions in a molten metal (Fuji's mechanism)

Fujii et al. [32] proposed a new mechanism of bubble generation, while again hydrogen is the major source of the porosity in aluminum alloys. They show that during electron beam welding, therefore under vacuum, the bubbles are formed through a reaction between the molten Al and Al2O3, forming Al2O gas (4 Al (l) + Al2O3 (s) => 3 Al2O (g)).

SUMMARY AND CONCLUSIONS

The mechanism by which porosity forms, even if not well understood, is undoubtedly related to the solidification mechanism of a given aluminum alloy system. The main mechanism responsible for the formation of porosity in aluminum alloys is clearly linked to the variation of solubility of hydrogen between the liquid and the solid state at the solidification temperature.

Aluminum welds and casts may contain porosity as a result of hydrogen-bearing contaminants. These contaminants, such as moisture or hydrocarbons are converted to atomic hydrogen and subsequently transferred into the molten pool in accordance to Sievert's law.

In order to nucleate porosity in welds and casts, a threshold value of hydrogen is required. The threshold value of porosity nucleation depends upon the alloy composition, the solidification kinetics and the welding or casting conditions, which one can control to effectively limit porosity problems in aluminum welds and casts.

Nuclei bubbles grow by hydrogen diffusion, and the main mechanism by which larger hydrogen bubbles grow during welding is coalescence of smaller bubbles by larger ones. Considering that shrinkage-voids (type of porosity present in casting) are excluded, most common types of porosity are spherical and interdendritic (irregularly shaped).

In the case of keyhole welding, welds may contain porosity as a result of gas entrapment by keyhole instability, which can be partly caused by the evaporation of magnesium contained in the base metal. Concerning arc welding and conduction mode welding, evaporation of magnesium might be another way of porosity formation by nucleation and growth; however the proof of its existence must be further demonstrated.

REFERENCES

[1] ASM International, “Aluminum Alloy Castings: Properties, Processes, and Applications”, product code 05114G, chapter 5 The influence and control of porosity and inclusions in Aluminum castings”, pp 47-54, available online at the following URL http://www.asminternational.org/pdf/spotlights/5114alum_castc5.pdf

[2] Diran Apelian, M.M Makhlouf, “High integrity aluminum die casting : alloys, processes and melt preparation”, NADCA item#307, April 2004.

[3] R.J. Shore and R.B. McCauley, “Effects of porosity on high strength aluminum 7039”, Weld. J., pp. 311s – 321s, July 1970.

[4] W.R. Opie and N.J. Grant, “Hydrogen solubility in aluminum and some aluminum alloys”, Trans. AIME, Vol 188, pp 1237-1241, oct 1950.

[5] R.A Woods, “Porosity and Hydrogen absorption in Aluminum welds”, welding research, supplement to the welding journal, pp 97-108, March 1974.

[6] Jean Charbonnier, “Gaz dans les alliages d’aluminium de fonderie”, techniques de l’ingénieur traité matériaux métalliques, section M218.

[7] D.Apelian, K.Tynelius, J.F.Major, “A Parametric Study of Microporosity in the A356 Casting Alloy System”, American Foudrymen’s Society (AFS), pp 402-413, 1994.

[8] R.P Martukanitz, P.R Michnuk, Sources of porosity in gas metal arc welding of aluminum, american society for materials, 1982.

[9] M.C Flemmings, Solidification processing, chapter 6, pp 203-210, McGraw-Hill Inc. (1974).

[10] S.D McDonald, A.K. Dahle, J.A. Taylor, D.H. StJohn, J.W. Zindel, “Microstructural evolution of an Al-Si-Mg foundry alloy during solidification”.J.C. Papritan , et al., in: L.P. Conner (Ed.), Welding Handbook, Vol.2, 8th ed.,AWS, 1987, p.336.

[11] J.P Anson, J.E Gruzleski, “Effect of Hydrogen content on relative shrinkage and gas microporosity in Al-7% Si casting”.

[12] A.Haboudou, P.Peyre, A.B Vannes, G.Peix, “Reduction of porosity content generated during Nd:YAG laser welding of A356 and AA5083 aluminum alloys”, Materials science and engineering, A363, pp 40-52, 2003.

[13] Kiyoshi Nogi, Yasuhiro Aoki, Hidetoshi Fujii, K. Nakata, “Behaviour of bubbles in weld under microgravity”, Acta materialia, vol 46, no 12, pp 4405-4413, july 1998.

[14] Lih-Ren Hwang, Chung-Hau Gung, Teng-Shih Shih, “A study on the qualities of GTA-welded squeeze cast A356 alloy”, Journal of Materials Processing Technology 116, pp 101-113, 2001.

[15] S.T. McClain, J.T. Berry and B. Dawsey, “A study of porosity and pore morphology in aluminum A356.2 Step castings”, American Foundry Society, 2003.

[16] Website http://www.key-to-metals.com

[17] J.H. Devletian and W.E.Wood, “Factors Affecting Porosity in Aluminum Welds – A Review”, welding research, supplement 290 to the welding journal, pp 1-18, December 1983.

[18] A.Haboudou, “Caractérisation, modélisation et maîtrise des porosités créées lors du soudage laser Nd-YAG d’alliages d’aluminium”, these ecole centrale de Lyon-CLFA, janvier 2003.

[19] O.N. Kudryashov,, V.I. Eliseev,V.S. Vinogradov, “Effect of preparation of components on weld porosity in welding 1201 aluminium alloy”, Welding International, vol.8, no.11. pp.916-917, Nov.1994.

[20] M. Pastor, H. Zhao, R.P. Martukanitz and T. Debroy; “Porosity, Underfill and Magnesium Loss during Continuous Wave Nd:YAG Laser Welding of thin Plates of Aluminum Alloys 5182 and 5754, Welding research supplement.

[21] J.C. Papritan , et al., in: L.P. Conner (Ed.), Welding Handbook, Vol.1, 8th ed.,AWS, 1987, p.7-8.

[22] Website http://www.weldingengineer.com

[23] Website http://airliquide.com/saf/chapter02/fr/notvent/productivite/9235_1.pdf, Air Liquide Welding, dossier procédé topmag tandem, Référence notice 15159235, Août 2001.

[24] BINGER, W.N. YANOK and MICHNUK, Internal Report ALCOA, Technical Center, 1975.

[25] M. Mazur, “Porosity in aluminum welds”, Welding International, vol.6, no.12. pp.929-931,1992.

[26] Matsuda, “Effect of electromagnetic stirring on weld” solidification structure of Aluminium Alloys Trans JWRI Vol 7 (2) 1978.

[27] J.M. Wheatley, “Significance of air entrainment through the filler wire conduit on the occurrence of porosity when welding aluminium” Australian Welding Research, vol.12. pp.47-48, Dec.1983.

[28] T. Shinoda, I. Masumoto, “Effects of chlorine additions [to shielding gas] on the occurrence of porosity in aluminium MIG welds”, Welding International, vol.3, no.12. pp.1034-1039, 1989.

[29] J.C. Papritan , et al., in: L.P. Conner (Ed.), Welding Handbook, Vol.1, 8th ed.,AWS, 1987, p.22.

[30] Websitehttp://www.saf-airliquide.com/fr/actus/exial2.htm#exemple

[31] L. Liu, G. Song, G. Liang, J. Wang, “Pore formation during hybrid Laser-TIG of Magnesium alloy AZ31B-Mechanism and remedy”, Materials science and Engineering A390, pp 76-80, 2005.

[32] J.C. Papritan , et al., in: L.P. Conner (Ed.), Welding Handbook, Vol.1, 8th ed.,AWS, 1987, p.21.

[33] Hidetoshi Fujii, Kiyoshi Nogi, Yasuhiro Aoki, Hideaki Umatoshi, “Bubble formation in aluminum alloy during electron beam welding”, Journal of Materials Processing Technology 155-156, pp 1252-1255, 2004.

[34] J.F. Lancaster, “Metallurgy of welding”, 3rd ed., allen and Unwin, Boston, Mass., pp254, 1980.

[35] Z.P. Saperstein,G.R. Prescott, E.W. Monroe, “Porosity in aluminum welds“, Weld. J., Vol. 43(10), pp443s-453s, 1964.

[36] J.M. Fortain et al., “Recent developments in arc welding with shielding gas of aluminium and its alloys” Welding International, vol.15, no.4, pp.294-300, 2001.

[37] B. Chalmers, “Principles of solidification”, John Wiley and Son, New York, pp319, 1967.

[38] M. Kutsuna, “Metallurgical aspects in laser welding of steels and aluminum alloys” Proceedings Icaleo 1996.

[39] J.C. Papritan , et al., in: L.P. Conner (Ed.), Welding Handbook, Vol.2, 8th ed.,AWS, 1987, p.336

[40] D.F. de Lange et al. “Unsteady Meltpool and Keyhole Modelling for Laser Welding”, (http://www.wa.wb.utwente.nl/Staff/deLange/CR2002k.html)

SECTION 3: EVALUATION OF POROSITY IN AL-SI WELDS FOR 3 DIFFERENT WELDING TECHNIQUES

INTRODUCTION AND BACKGROUND

The automotive industry is currently facing increasing demands to simultaneously improve its fleet average fuel economy and reduce greenhouse gas emissions. In order to meet these new standards, the industry is moving toward decreasing the weight of the vehicles through the use of new materials, especially lightweight aluminum alloys. One of the major factors in their implementation involves the ability to fabricate, easily and reproducibly, structurally sound and defect-free welds. Porosity, loss of alloying elements and, for some heat treatable aluminum alloys, solidification cracking are the most common problems encountered in the welding of these alloys. The detrimental effect of porosity on the mechanical properties of aluminum welds, and especially concerning fatigue, has been documented in the literature. However, the mechanism of porosity formation during welding is less well understood.

Three welding techniques have been selected: a laser/MIG hybrid process, a MIG dual wire welding process, and an electron beam welding process. The goal is to weld a rolled thick sheet of Aluminum alloy 5454 to an Aluminum alloy A356 cast part.

The section is divided into 4 parts.

After having introduced the subject in a first part, the second part rapidly presents the experimental methods that have been applied. The third part aims to analyze the main results of the experiments performed, and proposes porosity formation mechanisms related to each welding technique under investigation, taking in account the literature review and the experimental results. Finally, conclusion and perspectives are presented in a fourth part.

EXPERIMENTAL METHODS

Welded materials

The chemical composition of the materials under investigation is reported in the Table 1. The values under brackets are given in the ASM SPECIALTY HANDBOOK [1].

Table 1: Chemical composition of the materials under investigation

ALLOY	SI	MG	MN	CU	TI	FE	ZN
A356 (AS7G03)	6.8-7.5	0.2-0.45	0.35	0.25	0.25	0.6	0.35
5454	0.25	2.7	0.8	0.1	0.1	0.4	0.25
4043	4.5- 6)	0.05	0.05	0.3	0.2	0.8	0.1

Table 2: welding parameters

	Hybride Laser/MIG			
Parameters	Laser Nd:YAG	**MIG**	**Electron Beam**	**MIG dual-wire**
Welding speed	2,1 m/min		2 m/min	1,9 m/min
shielding gas	70% Ar, 30% He		Vacuum	Ar
shielding gas flow	20 L/min			
Welding current		240 A	110 mA	274 A / 240 A
Welding voltage		29 V	40 V	24,4 V / 25,2 V
Power	4 kW			
Wire feeding speed		11 m/min		(16 m/min) / (15 m/min)
transfert mode		axial spray		
stick out		18 mm		
Laser diameter	600 microns			
lens focal length	200 mm			
focusing intensity			1,82 A	
circular vibration			0,03 V	

Welding parameters

The welding parameters that have been applied during welding are reported in the Table 2 above.

Same welding speeds (1.63 m/s) have been applied for the 3 welding techniques. Shielding gas differs for each welding technique.

It should be noticed that the surface of the welded metal have not been prepared by using a same method. This could be a reason to explain the very different level of porosity in the welds. In the case of MIG welding, as well as in the case of the hybrid laser/MIG welding technique, the sheet has been previously machined to create a chamfer, and cleaned with acetone. Concerning the electron beam welding technique, the surface of the metals has been cleaned with acid alcohol (janitol), and no machining has been previously performed.

1st Analysis on the amount and the distribution of porosity in welds

The first step of this study was to have an idea about the amount of porosity that was present in the welds. Thus, Radiography experiments were firstly performed. In a

second time, it was necessary to transversal cut the welds and to observe the porosity in more details by optical microscopy.

Definitions

This detection limit of the X-Radiography (300 microns) has lead to define the terms microporosity and macroporosity. Indeed, micropores are pores whose diameter is lower than 300 microns, whereas macropores present a diameter greater than 300 microns. These two definitions are widely used in the literature.

An other important definition, which is the index used to characterize the porosity, is the % porosity, defined as:

$$\%\ \text{porosity} = \frac{\sum(\text{surfaces of the pores})}{\text{cross section surface of the weld}} \quad (1)$$

X-Radiography

First of all, X-Radiography has been carried out on the sample, aiming to a first characterization of the porosity for all the welding techniques considered.

The limit of detection of the X-radiography, knowing that the thickness of the samples is fixed, is 0.3 millimeters. Therefore, pores whose diameter is greater than 300 microns can be detected through X-radiography, but pores whose diameter is lower than 300 microns will not appear on the film.

The parameters used in X-radiography are represented in the Table 3 below:

Table 3: X-Radiography parameters used

Voltage	Current	Time
80 kV	5 mA	1 minute

Machining: Seifert ERESCO MF1 (Tube MIR 200E, 200kV; 4.5 mA; 900W)

Optical Microscopy

X-Radiography gave a global approach concerning the detection of porosity.

Optical microscopy let a finer, but more localized detection. Thank to optical microscopy, pores whose diameter was greater than 300 microns could be easily detected.

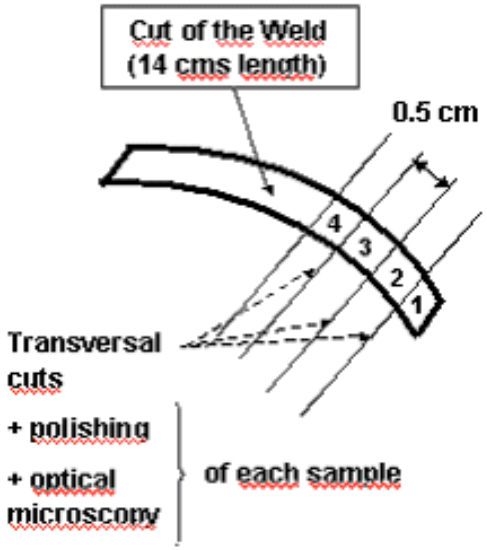

Figure 18: transversal cuts for metallurgical examination

Using these cuts, we went through different steps to finally characterize the porosity in the welds. These different steps are represented in the table 4 below:

Table 4: steps applied to the porosity detection by optical microscopy

STEP NUMBER	DESCRIPTION
1	Transversal cut with a 1 mm thick alumina disc (see Figure 18) Cutting machine: Buehler ABRASIMET II
2	Metallographic preparation before microscopic examination: Polishing thanks to grinded SiC paper, alumina and diamond. The samples were not etched. Polishing tables: Mecapol P255 U2 / P320 / AUTOMATIQUE
3	Optical microscopy pictures of the weld were taken according to the defined grid (see chosen grid for each process on Figure 19) Macroscope: Leica MZ125, Microscope: Leica MEF4M
4	The sizes of porosity were measured by a software. Software : Leica IM1000

Using the microscopy pictures, the level of porosity was determined for each of the studied welding techniques.

Because the welds beads present different shapes, a grid has been defined differently for each welding process under investigation (Figure 19). It should be noticed that no grid has been defined for the electron beam welding technique whose porosity distribution was not under evaluation due to the reduced amount of porosity present in the welds.

Figure 19: Grids used to define parts letting study the porosity distribution

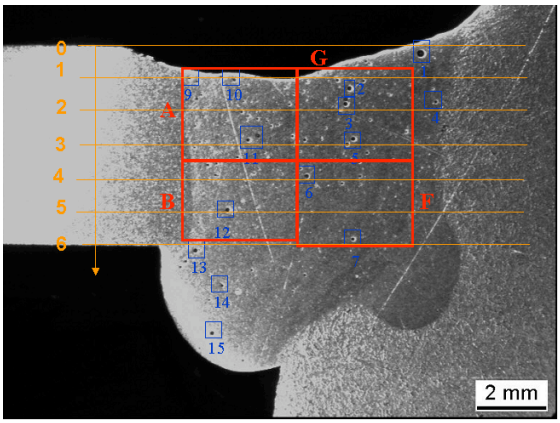

(a) Grid used for the MIG welding process

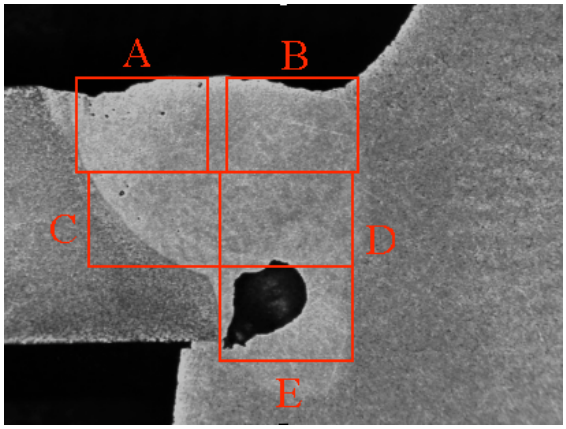

(b) Grid used for the Hybrid welding process

2nd analysis: Solidification of the welds

Aiming to analyze the solidification characteristics of the weld, many experimental investigations have been performed. The first one is an analysis of microstructure by optical microscopy. To complement, a micro-hardness evaluation has been performed inside and outside of the weld. Finally, an analysis of the chemical composition variation inside the weld has been carried out.

Microstructure analysis by optical microscopy

Concerning the microstructure analysis, a similar metallographic preparation has been performed. In order to reach the best conditions of microstructure observations, different etching techniques have been evaluated and the best has been selected.

The different steps are represented on the Table 5 below:

Table 5: Method applied to microstructure analysis

STEP NUMBER	DESCRIPTION
1	Transversal cut with a 1 mm thick alumina disc (see Figure 18) Cutting machine: Buehler ABRASIMET II
2	Metallographic preparation before microscopic examination: Polishing thanks to grinded SiC paper, alumina and diamond. Polishing tables: Mecapol P255 U2 / P320 / AUTOMATIQUE
3	Etching: The samples are placed/immersed into the acid solution* for 5 seconds, and then rinsed with water and dried, before examination through optical microscopy Macroscope: Leica MZ125, Microscope: Leica MEF4M
4	Dendrite arm spacing and cell sizes were measured by a software. Software: Leica IM1000

**Chosen etching chemical reactant: acid solution (non diluted) made of:*

- *Poulton Reactant (50 mL)*
  - *–12 mL HCl concentrate*
  - *–6 mL HNO3 concentrate*
  - *–1 mL HF (48%)*
  - *–1 mL H2O*
- *HNO3 (25 mL)*
- *12 grams of chromic acid dissolved into 40 mL of water*

Different zones have been identified, called as columnar and equiaxed zones (see definitions in glossary).

It has unfortunately been sometimes impossible to detect dendrites in certain parts of the welds equiaxed zones. This was probably due to a high convection in these mentioned parts inside the molten bead during solidification.

Micro-hardness and electron microprobe analysis

For each welding technique, the experimental steps that have been performed are explained in Table 6.

Table 6: Experimental steps performed for micro-hardness and EDX

STEP NUMBER	DESCRIPTION
1	Transversal cut with a 1 mm thick alumina disc (see Figure 18) Cutting machine: Buehler ABRASIMET II
2	Metallographic preparation before microscopic examination: Polishing thanks to grinded SiC paper, alumina and diamond. The samples were not etched. Polishing tables: Mecapol P255 U2 / P320 / AUTOMATIQUE
3	Micro-hardness analysis Machine: Buehler MICROMET II
4	EDX analysis Scanning Electron Microscope (SEM): Jeol JSM 6400 EDX: Oxford instruments 6506

In the case of the MIG and the laser hybrid welding techniques, EDX analysis has been performed along the lines defined by the micro-hardness holes; each EDX measurement has been carried out between 2 holes. This remark doesn't apply concerning the electron beam welding process, because the EDX analysis of electron beam welded samples has been performed before the micro-hardness analysis.

RESULTS AND DISCUSSION

Results of the 1st analysis: Amount and distribution of porosity in welds

X-Radiography results

Assessment of the radiography results

Radiography results are reported in the Table 7 below:

Table 7: Radiography results

Welding process	Electron beam	MIG dual-wire	Hybrid Laser/MIG
Porosity detection	No detection	No detection	Many pores uniformly distributed

No porosity has been seen on the films neither in the case of electron beam welding nor in the case of MIG dual wire welding.

Nevertheless, many pores have been observed in the case of the laser hybrid welding process. Macrocavities (or macroporosity) are present in the Laser hybrid welds only.

Case of the Laser/MIG hybrid process: comparison with standards

In the case of the laser hybrid process, many macropores have been observed on the radiographic film. We have been able to measure the size of the pores on the film within a representative section of the radiographic film. Based on this data, it has been possible to compare the obtained level of porosity with quality standards. Results of this comparison with standards are reported in the Table 8 below:

Table 8: Laser hybrid – Porosity evaluation according to standards

Standard	criterion of acceptance	Acceptance levels (from best to worst)	Result
A89-220	θ *	E,1,2	Class 2 not respected
A89-220	Maximal diameter of the pores	E,1,2	Class 2 not respected
A89-232 (ISO 10042) For arc welding	Maximal diameter of the pores	B,C,D	D (weak requirement)
A89-234 (ISO 13919-2) For laser welding	Maximal diameter of the pores	B,C,D	C (moderate requirement)

$$* \ \theta = \frac{\sum (surface\ of\ the\ pores)}{surface\ of\ the\ weld\ bead}$$

The standards confirm that the hybrid laser/MIG welds present a high level of porosity.

Optical microscopy results

Electron beam welding process

In the case of the electron beam welding process, 6 cuts have been performed. Below on Figure 20 is represented a representative cut:

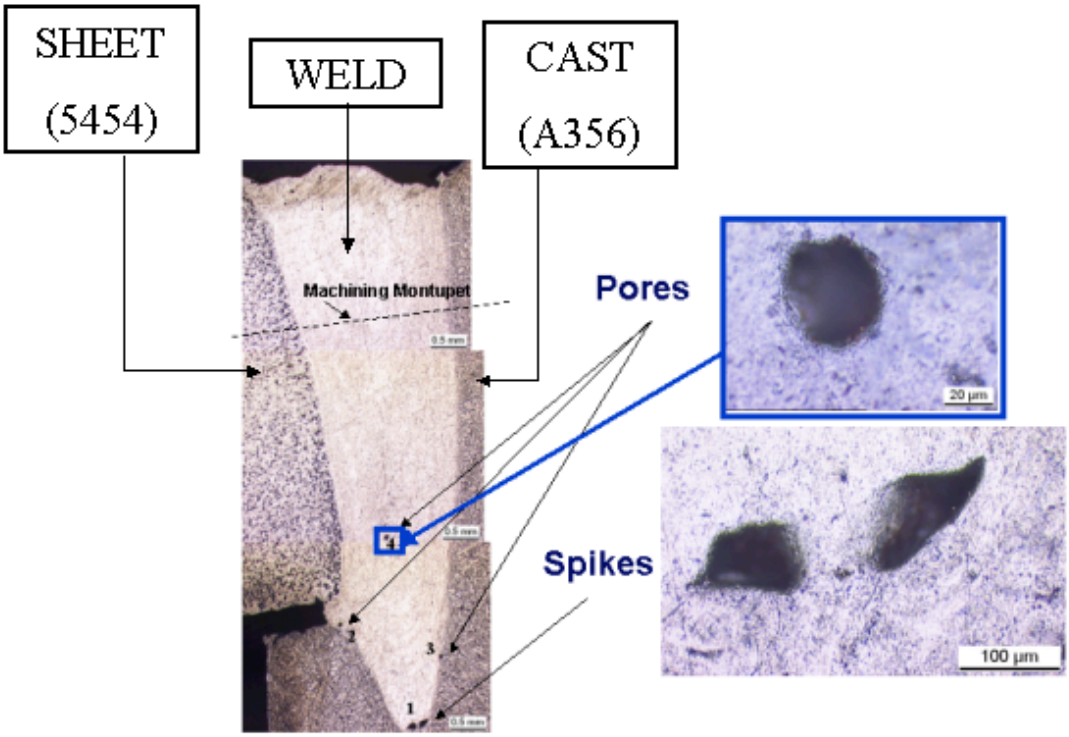

Figure 20: Representative electron beam weld

A few pores are present on this transversal cut (number 2,3,4). On the 6 cuts examined by optical microscopy, the pores have a diameter lower than 80 microns.

The amount of porosity (%porosity see equation (3)) has been estimated to be lower than 0.1 %. This amount of porosity is too low to consider a specific porosity distribution.

At the bottom, a special kind of porosity, called “spike”, is present on this cut, due to gas entrapment caused by the rapid solidification.

MIG dual wire welding process

In the case of the MIG welding process, 6 cuts have been performed. 2 of the 6 cuts presented a negligible porosity, and for this reason they have not been

taken into account concerning the porosity distribution analysis. Out of the 6 transversal cuts, the average of the porosity level has been estimated to 1.3%.

Below on Figure 21 is represented a transversal cut presenting many pores. In addition to the grid, a vertical axis named “DEPTH” was defined. We were then able to study the distribution of the porosity on the transversal cut, along this “DEPTH” axis in one hand, and on an other hand comparing the porosity present in the sheet side versus the porosity present in the cast side.

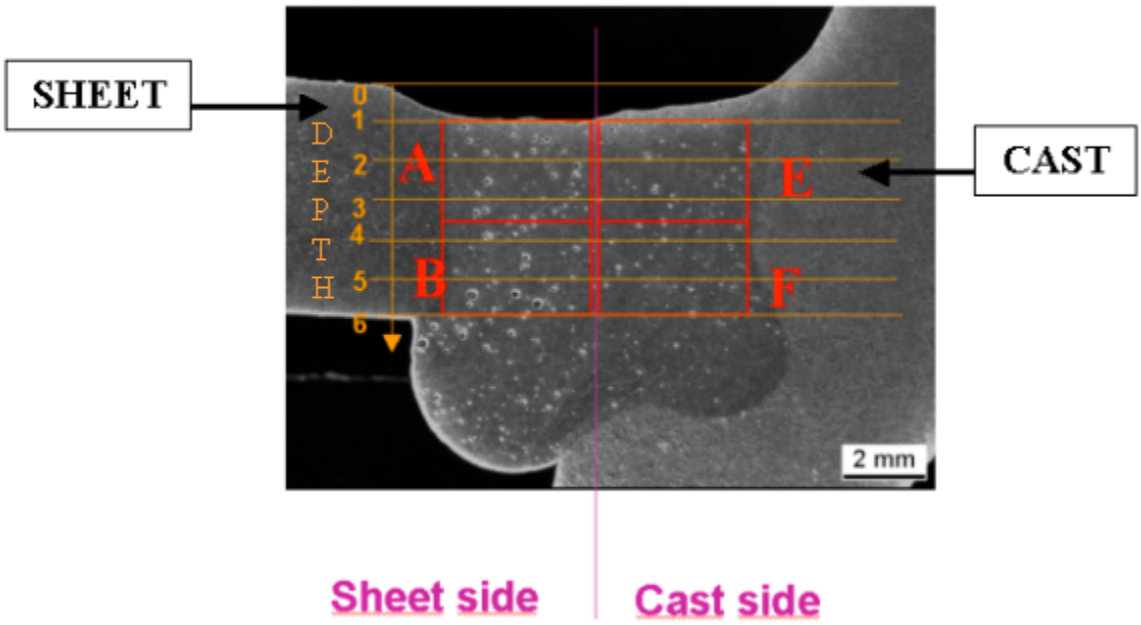

Figure 21: Porosity on a transversal cut of a MIG weld (3d cross section)

The assessment of porosity distribution along the “DEPTH” axis is plotted on the Figure 22 below:

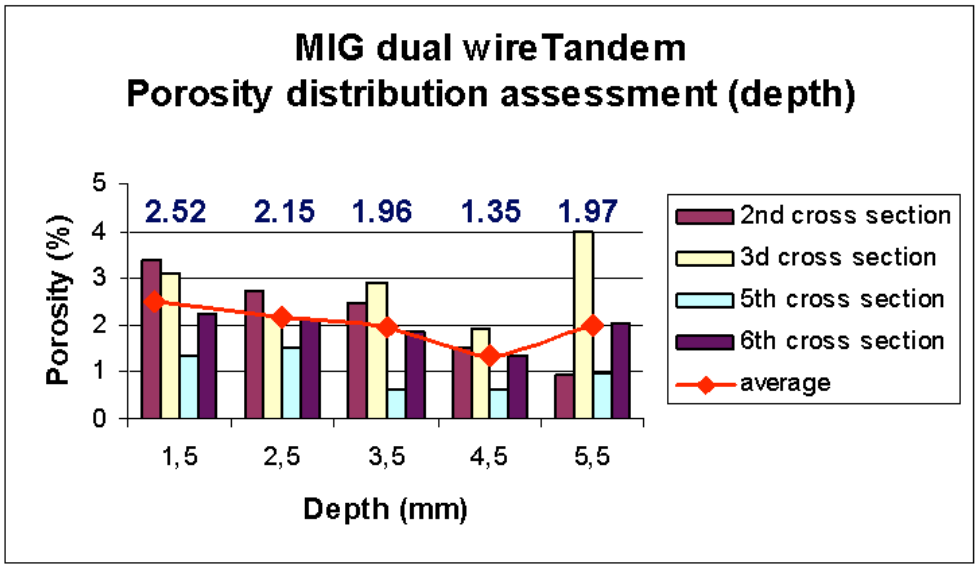

Figure 22: MIG - Porosity distribution assessment in depth

Out of the 4 transversal cuts presenting a non-negligible amount of porosity, the average level of porosity equals 2 %.

On the Figure 22 we observe that the level of porosity varies between 1.35% at 4.5 mm in depth to 2.52% at 1.5 mm at the top of the weld.

In addition, the assessment of porosity distribution along the width of the weld is represented on the Figure 23 below:

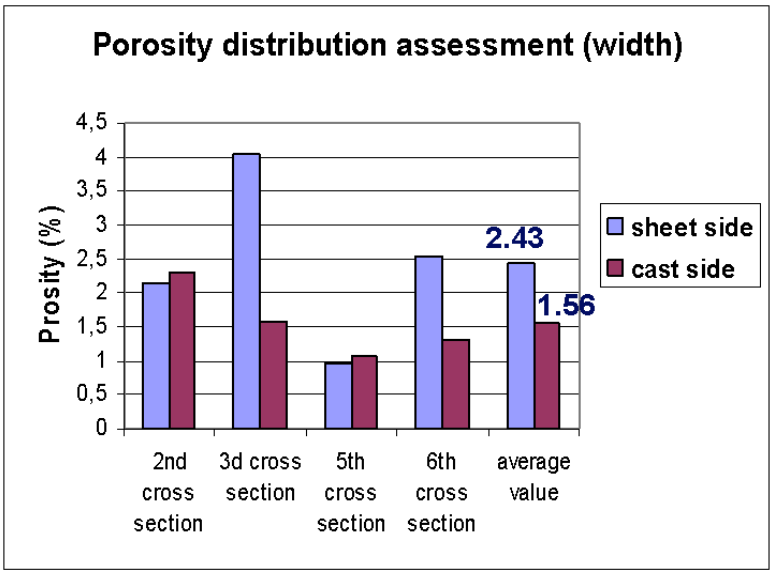

Figure 23: MIG- porosity distribution assessment in width

It is to observe that the level of porosity is more important on the part close to the sheet than on the part close to the cast (2.43% compared to 1.56%).

Hybrid Laser/MIG welding process

In the case of the hybrid laser/MIG process, 10 transversal cuts have been performed. Porosity in these 10 cuts has been evaluated and taken into account in the assessment presented in this part.

Level of microporosity versus macroporosity

The levels of macroporosity and microporosity are compared in the Figure 24 below:

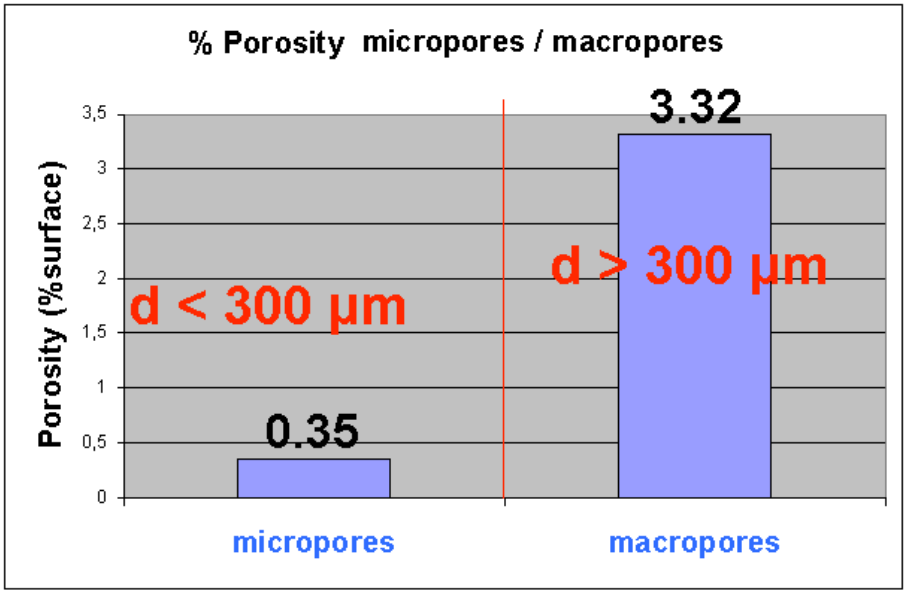

Figure 24: Hybrid Laser/MIG - level of macroporosity versus microporosity

Because of the large size of the macropores, microporosity content (0.35%) is almost negligible compared to the macroporosity content (3.32%).

Distribution of macroporosity

The distribution of macroporosity in depth is represented in the Figure 25 below:

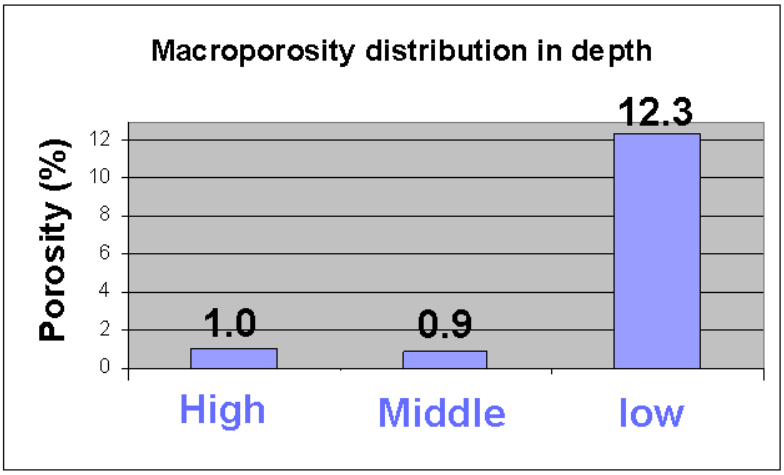

Figure 25: Hybrid Laser/MIG - Macroporosity distribution in depth

Most of the macroporosity is located in the lower part of the weld. It should be noticed that it has been observed that the macroporosity is located close to the edges of the weld.

Distribution of microporosity

The distribution of microporosity in depth is represented in the Figure 26 below:

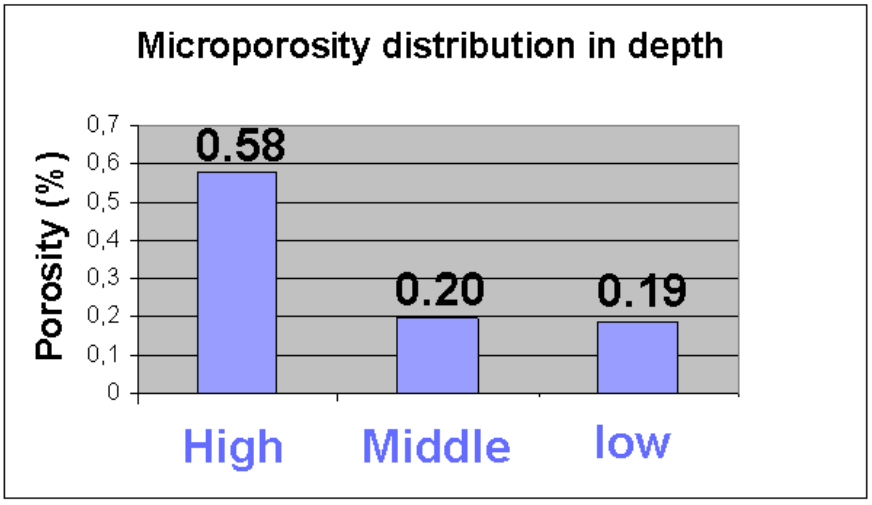

Figure 26: Hybrid Laser/MIG - Microporosity distribution in depth

Conversely, most of the microporosity is segregated in the upper part of the weld.

In addition, results of porosity distribution in width are represented in the Figure 27 below:

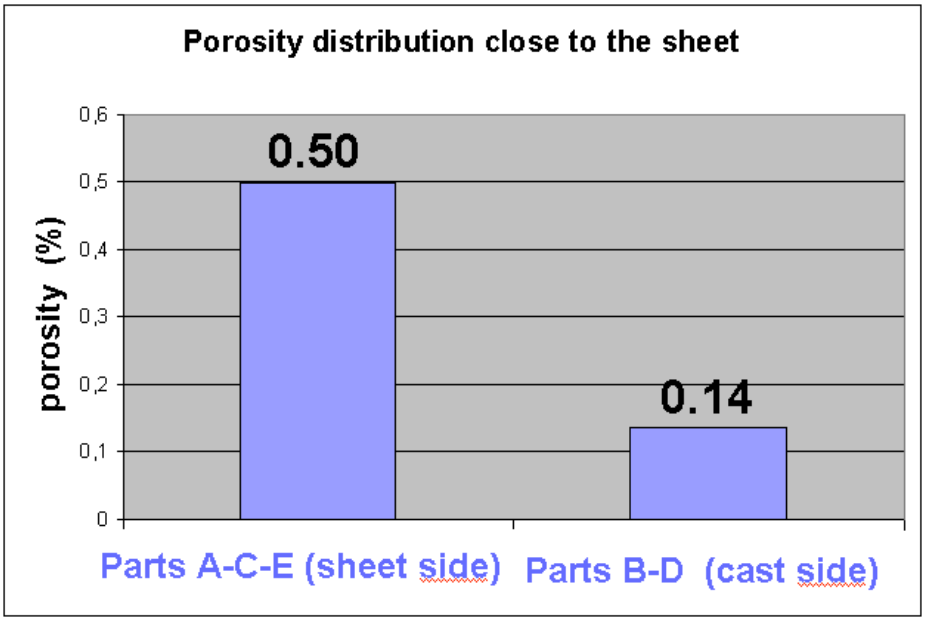

Figure 27: Hybrid laser/MIG – Microporosity distribution in width

Similarly to the MIG welding process, it is to observe that the level of porosity is more important on the part close to the sheet than on the part close to the cast.

Results of the 2nd analysis : Solidification analysis

Microstructure analysis: Optical microscopy results

Description of the observed microstructure

In this part, the microstructure of the cast, the sheet and the weld will be described based on the example of an electron beam welded sample.

Different types of microstructures

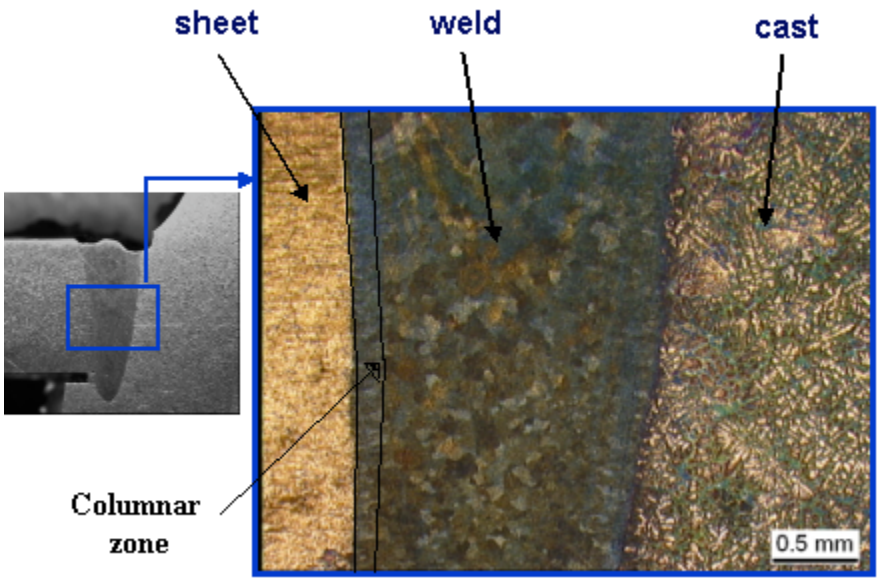

Figure 28: Microstructure of the Electron beam weld

On the figure above, we clearly can distinguish the weld between the sheet and the cast, the three of them presenting different types of microstructure.

On the left, the sheet presents a microstructure oriented in the rolling direction (Figure 29).

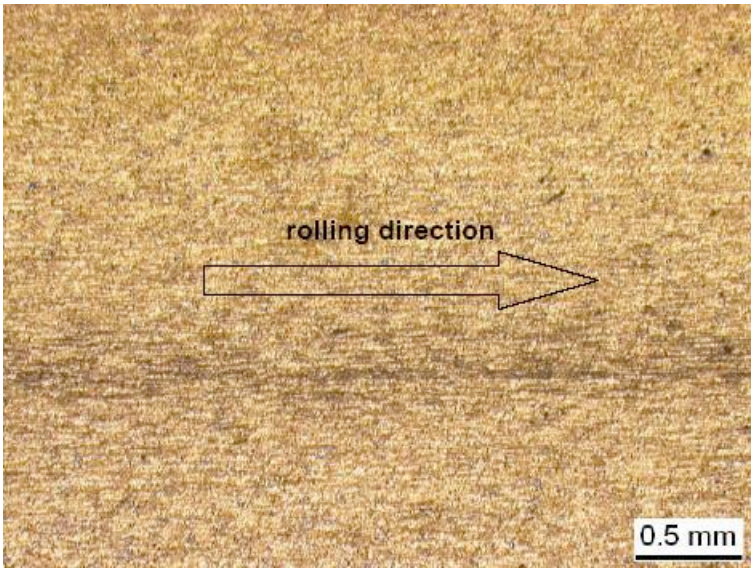

Figure 29: Microstructure of the sheet

On the right, the cast presents a dendritic structure (Figure 30):

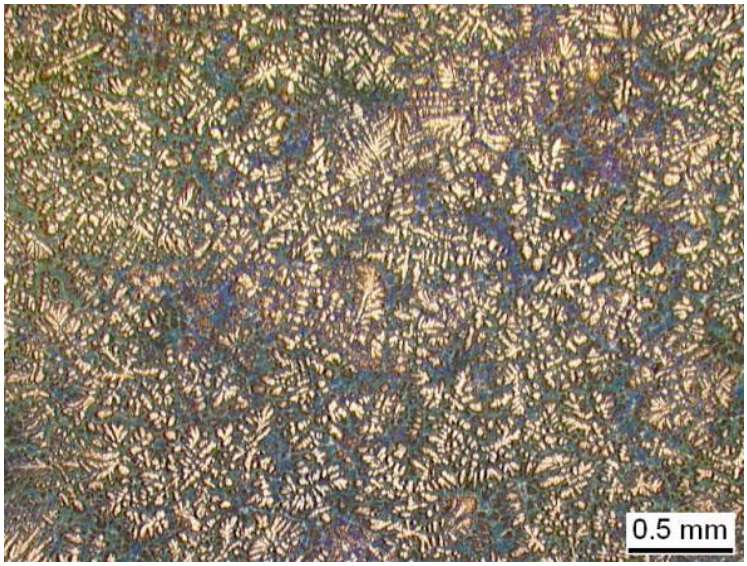

Figure 30: Microstructure of the cast

The average dendrite arm spacing (DAS) of the cast is estimated to 30 microns.

Finally, we can see that the weld presents small grains, which in fact correspond to smaller equiaxed grains oriented in a particular direction (Figure 31).

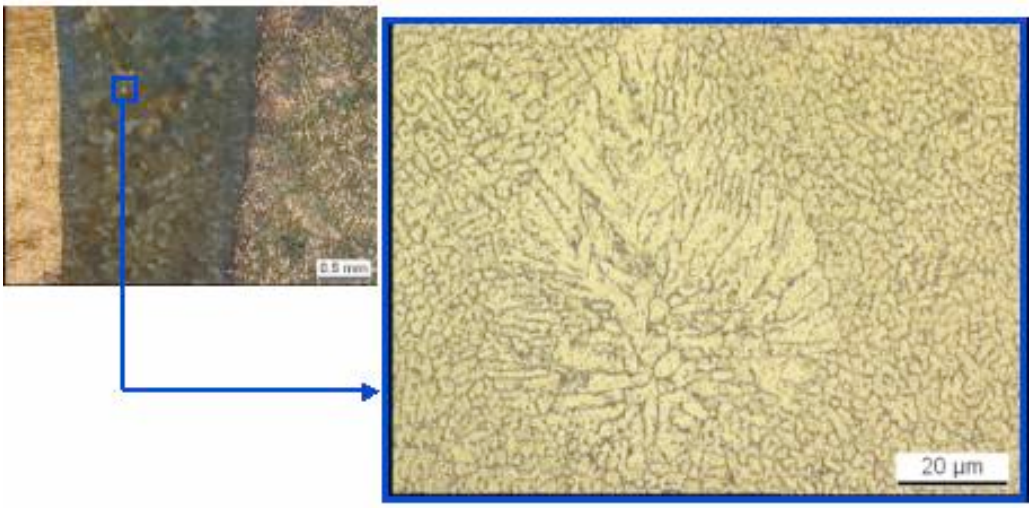

Figure 31: microstructure of the weld

Microstructure of the weld

At the edges of the weld, we can distinguish a zone, which is composed of columnar grains. The Figure 32 below shows columnar grains at the weld/cast interface.

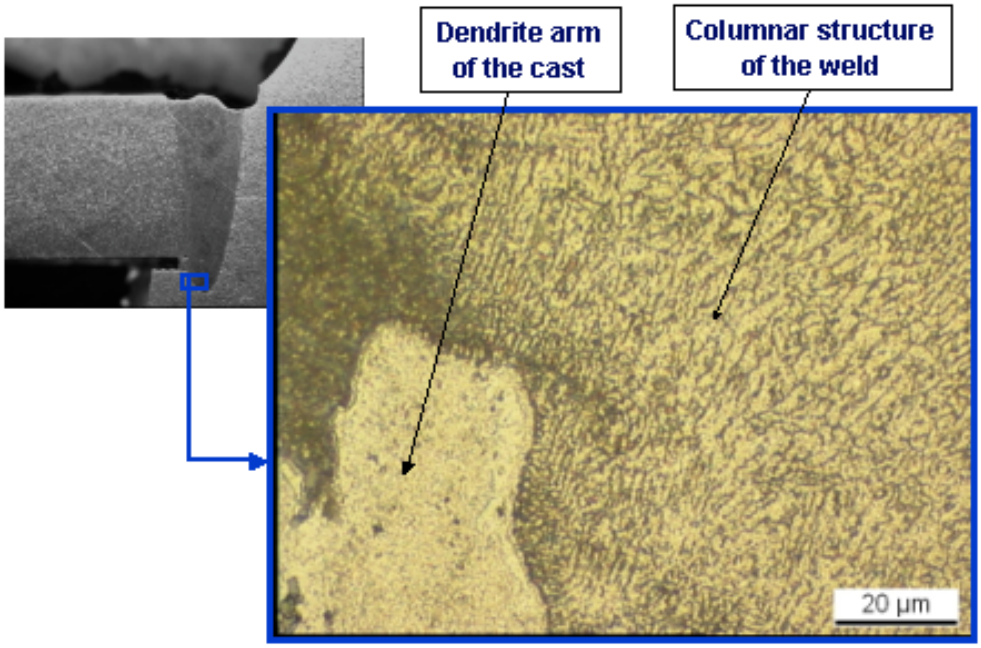

Figure 32: Microstructure at the bottom of the weld

At the sheet/weld interface also, a columnar structure appears clearly (Figure 33 on the left of the weld). The width of the columnar zone at this interface is around 180 microns.

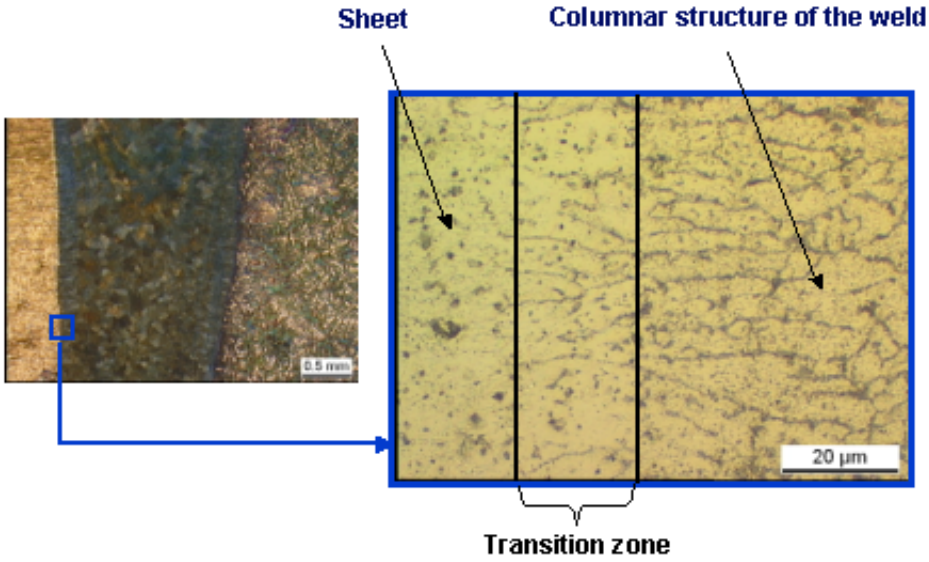

Figure 33: Microstructure of the interface weld/sheet

It should be noticed that between the sheet and the columnar zone, we can distinguish a transition zone. This phenomenon is observed on a length of 20 microns.

The size of the columnar zone depends on the convection in the weld bead and also on the welding speed. Greater the welding speed and the convection, smaller will be the columnar zone [2].

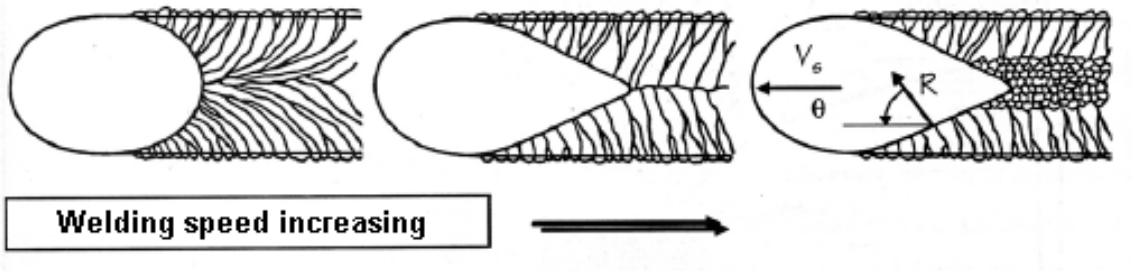

Figure 34: Microstructure of a weld versus the welding speed [2]

Different sizes of microstructure inside the weld

The weld shows different sizes of microstructure. It is well known that the smallest microstructure corresponds to the most rapid solidification.

The Figure 35 below shows an example of microstructure in the upper part of the weld. In comparison, the Figure 36 shows an example a microstructure in the lower part of the weld.

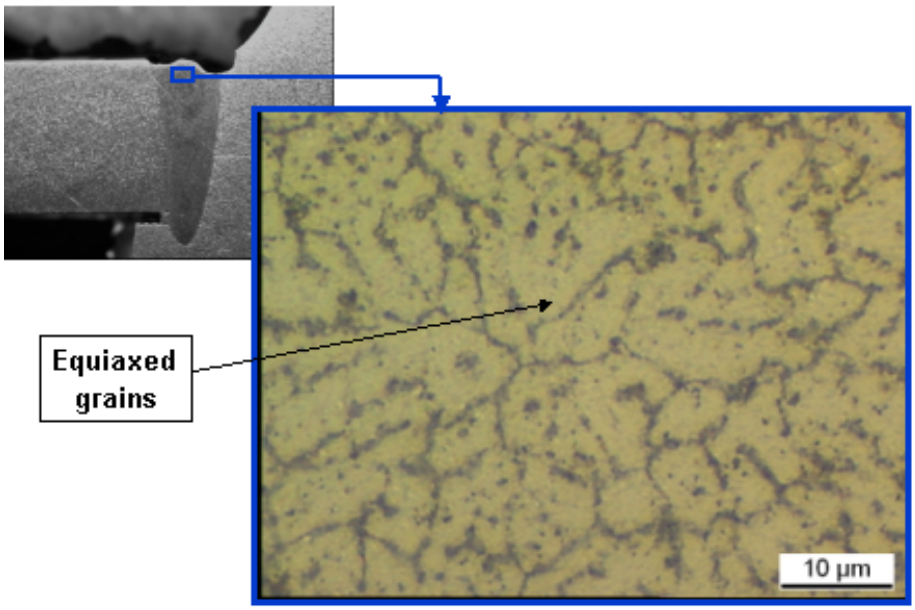

Figure 35: Microstructure in the upper part of the weld

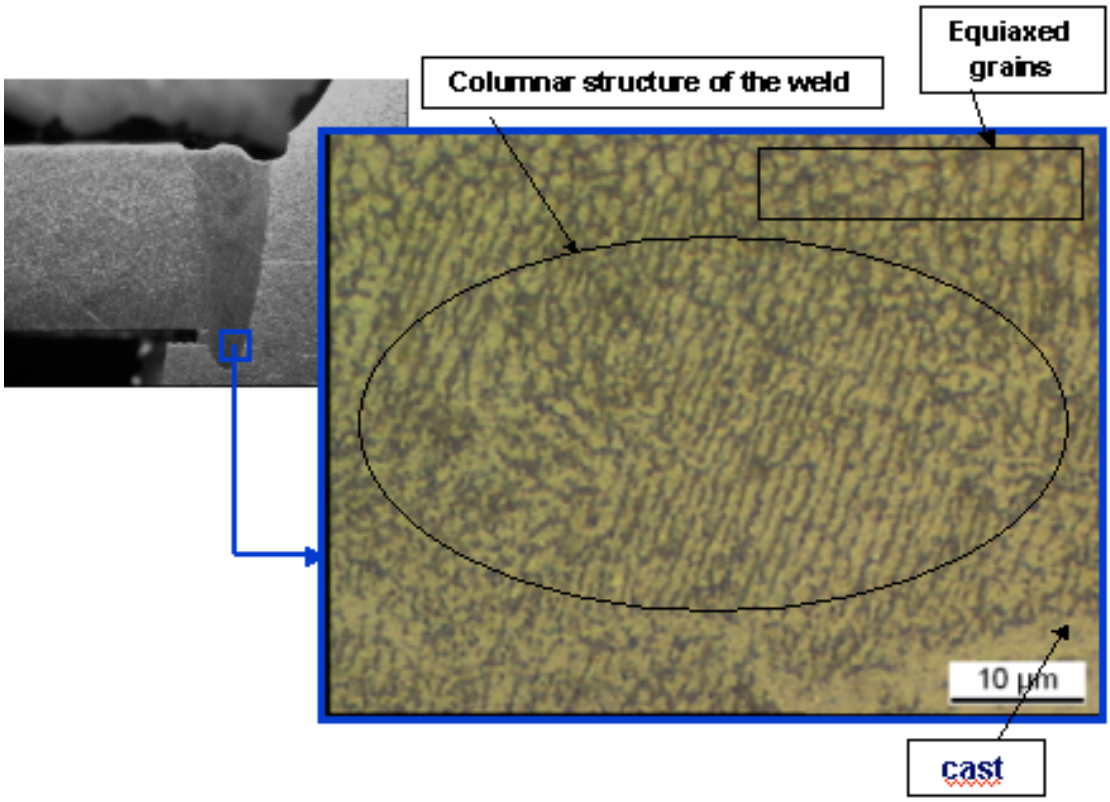

Figure 36: Microstructure in the lower part of the weld

We observe that the lower part of the weld presents a much finer microstructure than the upper part of the weld. It can be deduced from this observation that the weld has solidified more rapidly in the lower part than in the upper part.

Conclusions on the microstructure observation

The observation of the microstructure has lead to several conclusions:

- The weld has a columnar structure near in the zones close to the cast and close to the sheet. Equiaxed grains are present everywhere else.
- The grains of the weld show different microstructural orientation.
- The Weld's microstructure is coarser in the upper part of the bead, and in the center, as it is finer in the regions located close to the cast and close to the sheet.

- The microstructure is much finer in the weld than in the cast.

Solidification characterization by DAS and cell sizes measurement

Knowing that the microstructure of the weld presents different sizes, it was proposed to analyze this microstructure, aiming to understand more about the solidification process. The dendrite arm spacing has been chosen as microstructure index. This index let us calculate the local solidification times in different parts of the weld. Several formulas have been found in the literature, they are given in the Table 9 below:

Table 9: Equations letting calculate the local solidification time

$DAS = 5.5 \times (4.10^{-18} t_{local\ solidification})^{1/3}$ (4)		[2]
$DAS = A \times (t_{local\ solidification})^{N}$ (5)	A = 10; N=1/3	
$DAS\ (\mu m) = -7 + 12.5 \times (t_{local\ solidification})^{0.33}$ (6)		[3]

Method of investigation

Secondary dendrite arm spacing (DAS) measurements, as well as measurements of cell sizes in the equiaxed zones, have been carried out along horizontal and vertical lines which were specifically defined and drawn for each welding technique. Each line has been divided into 12 parts, and a measurement was performed in each part.

For every welding technique, the parts have been classified as follows:

- Horizontal lines: The part 1 is located close to the sheet, and the part 12 is located close to the cast.

- Vertical lines: The part 1 is located at the bottom of the weld, and the part 12 is located at the top of the weld.

A dendrite arm spacing measurement consists in measuring the total length from the center of the first dendrite arm (at the bottom of the “Christmas tree”) to the center of the last dendrite arm (“at the top of the Christmas tree”), and to divide this length by the number of secondary arm mines one. The obtained measured value corresponds in fact to the average of dendrite arm spacing.

MIG welding technique

Concerning the MIG welding technique, dendrites arms have been observed by optical microscopy on the total surface of welds transversal cuts.

Several lines have been defined within the weld, and the DAS has been measured along these lines.

The position of these lines is represented on the Figure 37 below.

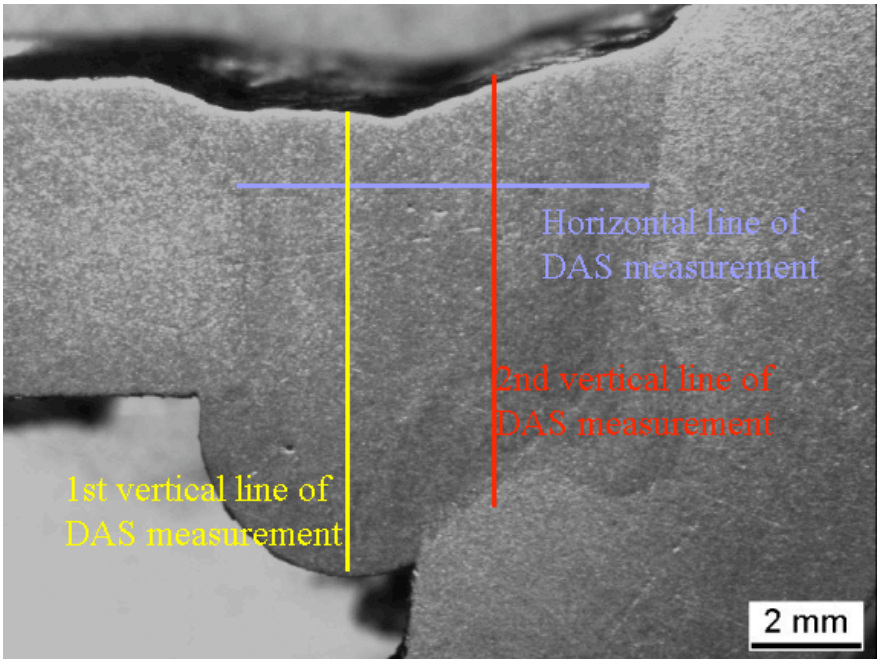

Figure 37: Position of direction lines for DAS measurements

Electron beam welding technique

In the case of the electron beam welding technique, the solidification has been characterized by dendrite arm spacing measurement along a horizontal axis at the edges of the weld and by cell sizes measurements along a vertical axis at the center of the weld, as represented in the Figure 38 below:

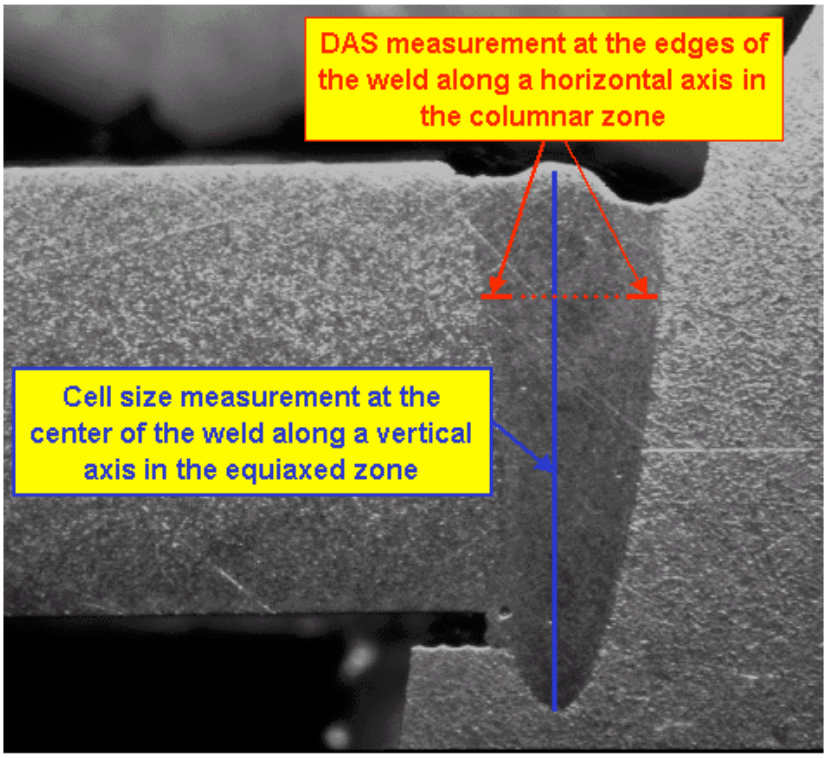

Figure 38: Location of DAS and cell sizes measurements

- *Dendrite arm spacing measurements*

It has been possible for the electron beam welds to measure values of dendrite arm spacing according to the method explained above and to characterize the local solidification time only in the columnar zones close to the edges of the weld. This investigation has been unfortunately impossible in the equiaxed zone at the center of the weld. This is probably due to the high convection (Marangoni

convection mainly according to P.D. Lee [3] of the molten metal breaking dendrites during solidification.

Dendrite arm spacing measurements have been performed in the columnar zone close to edges as shown in the Figure 38 above.

- *Cell size measurements*

Dendrite arm spacing measurements have been impossible in the center of the weld. Nevertheless, in this equiaxed zone, cell sizes have been measured.

The method of cell sizes measurements consists in:

- Dividing the vertical axis in 30 parts
- Taking pictures by optical microscopy in interesting parts within the vertical axis defined
- Defining a square presenting characteristic size of cells
- Counting and adding
- The number of entire cells inside the square
- The number of cut cells and divide this number by 2
- Plotting the obtained value versus the different parts numbers (see results on Figure 44)

Hybrid Laser/MIG welding technique

Concerning the laser hybrid welding technique, DAS measurements have been performed along a horizontal line (see Figure 39 below).

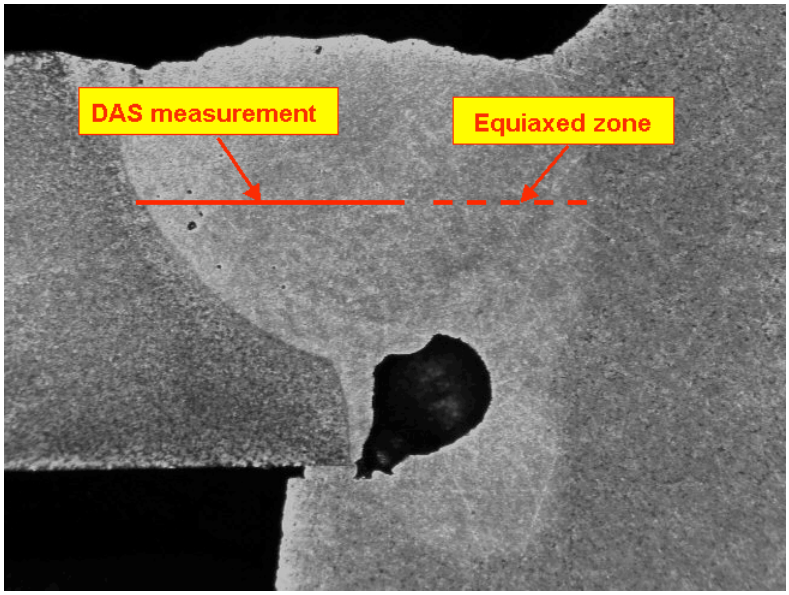

Figure 39: Index of microstructure for the hybrid technique

Results of DAS measurements

MIG dual wire welding technique

The results of secondary dendrite arm spacing measurements in the MIG dual wire welds are represented in the Figure 40 below:

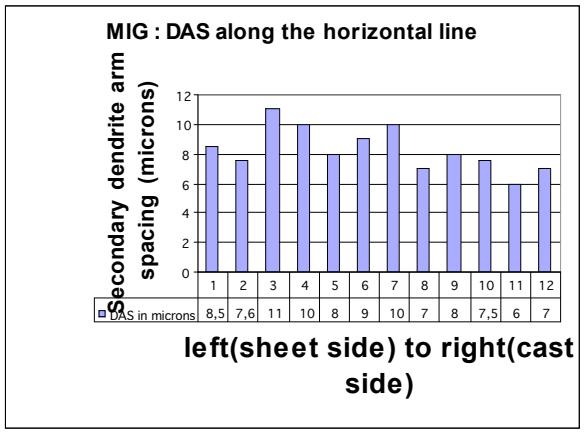

(a) DAS along the horizontal line

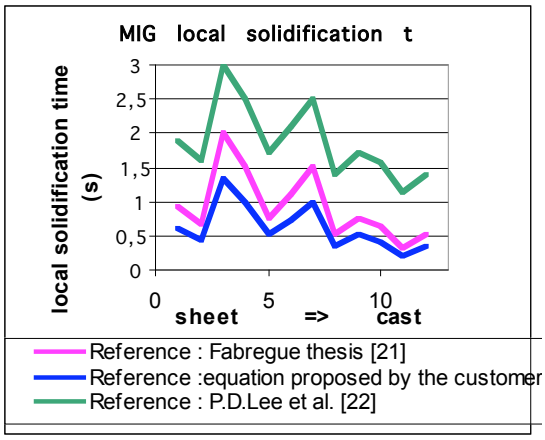

(b) Local solidification time along the horizontal line

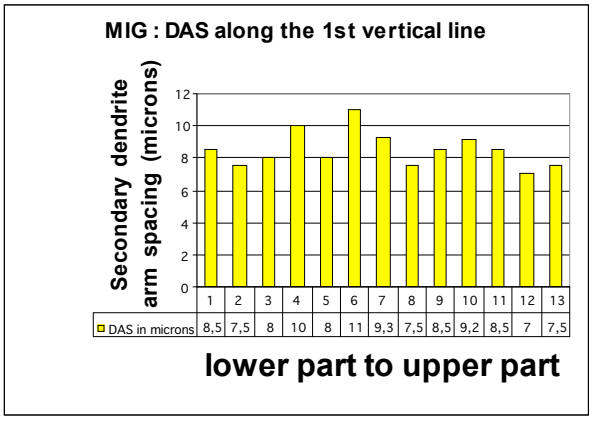

(c) Along the 1st vertical line (closer to the sheet)

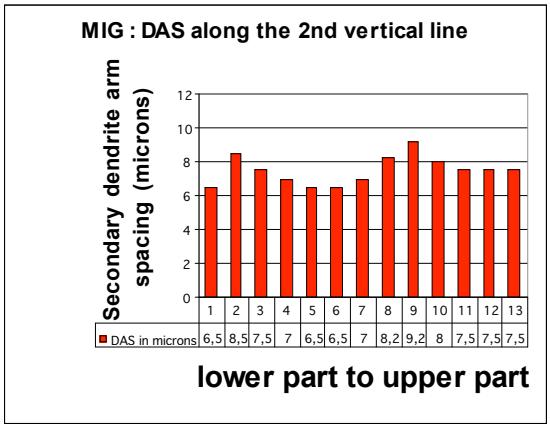

(d) Along the 2nd vertical line (closer to th cast)

Figure 40: MIG - Results of the DAS measurements

The average of dendrite arm spacing measured inside the MIG welds is 8.1 microns.

It should be noticed that the average dendrite arm spacing along the 1st vertical axis closer to the sheet (8.3 microns) is greater than the average dendrite arm spacing along the 2nd vertical axis closer to the cast (7.5 microns). This remark could lead to think that the solidification was more rapid close to the cast than close to the sheet.

It also appears that solidification was more rapid at the edges of the weld than at the center of the weld.

Concerning the DAS measurement along the vertical, the results are quite homogeneous and not enough significative to lead to any conclusion.

Electron beam welding technique

The results of secondary dendrite arm spacing measurements in the electron beam welds are represented in the Figure 41 below:

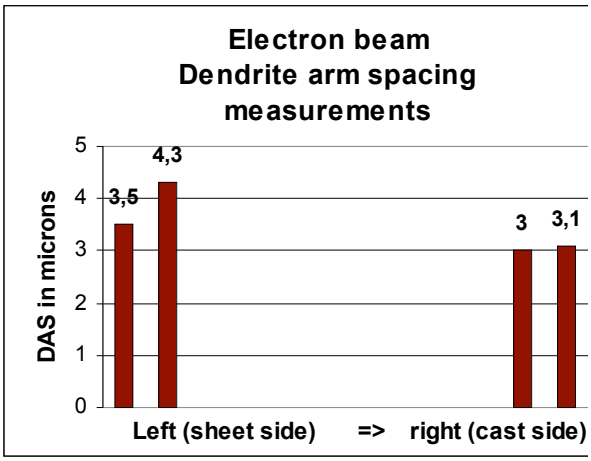

(a) DAS along the horizontal line

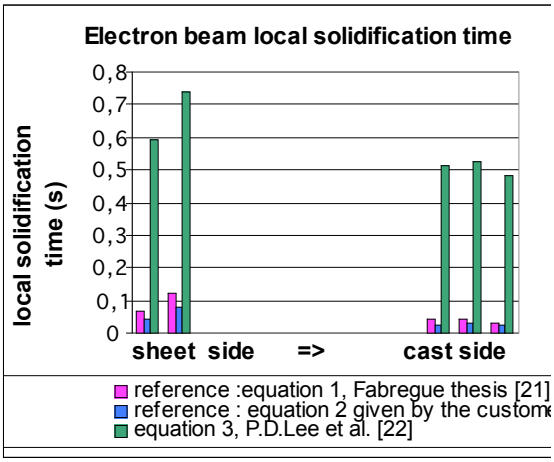

(b) Local solidification time along the horizontal line

Figure 41: Electron beam – Results of DAS measurements

The average of dendrite arm spacing measured inside the electron beam welds is 3.3 microns.

It appears again that the dendrite arm spacing, as well as the local solidification time, is smaller in the part close to the cast than in the part close to the sheet.

Hybrid laser/MIG welding technique

The results of secondary dendrite arm spacing measurements in the hybrid laser/MIG welds are represented in the Figure 42 below:

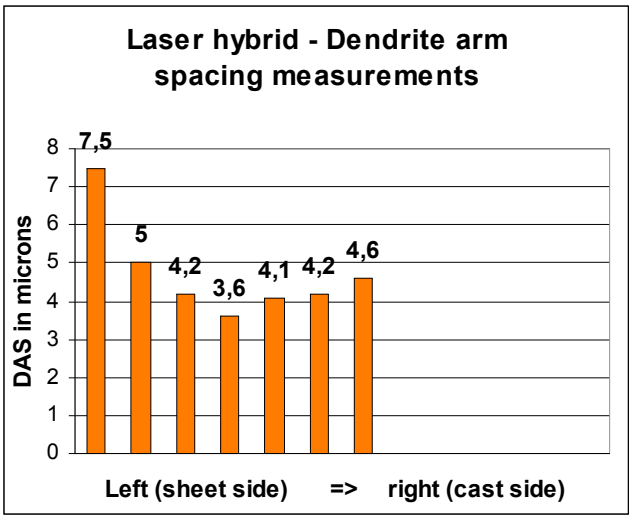

(a) DAS along the horizontal line

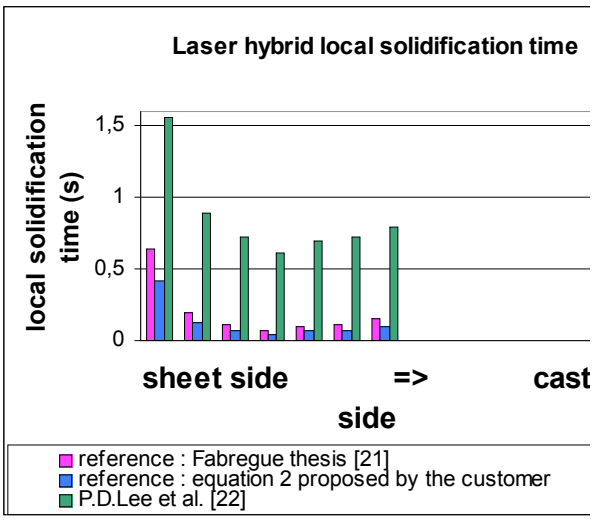

(b) Local solidification time along the

horizontal line

Figure 42: Hybrid Laser/MIG: Results of DAS measurements

The average of dendrite arm spacing measured inside the electron beam welds is 4.7 microns.

Comparison of the 3 techniques

Aiming to compare the types of solidification concerning the three selected welding techniques, the secondary dendrite arm spacing has been chosen as index, and the local solidification time as been calculated with the equation (3).

In the Figure 43 below, the obtained results are compared:

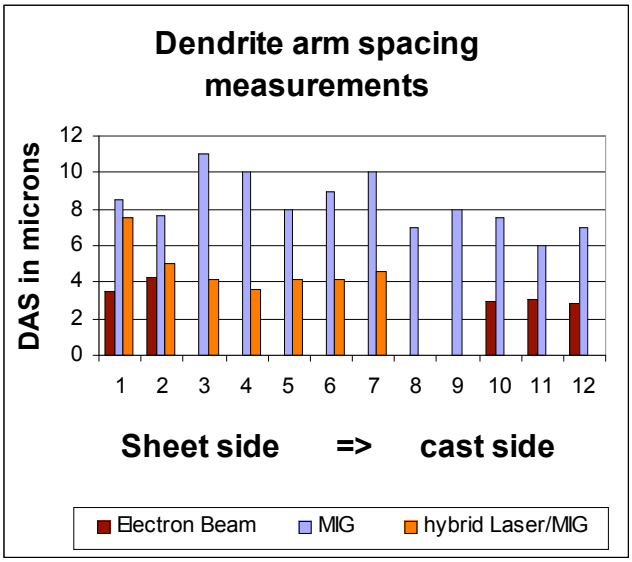

(a) DAS along horizontal lines

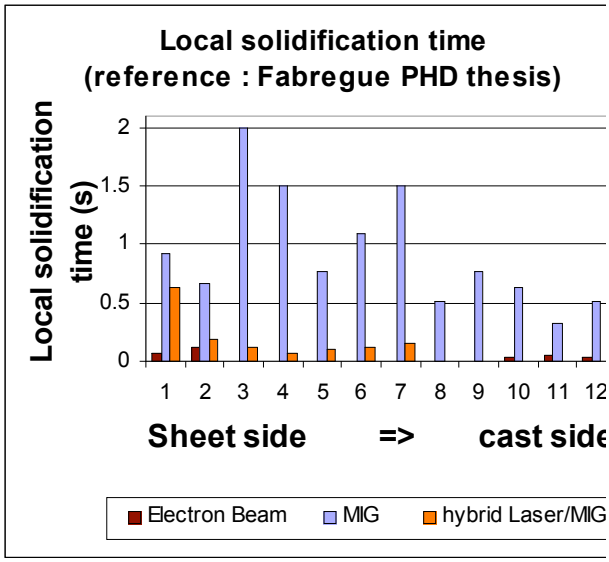

(b) Local solidification time along the horizontal lines

Figure 43: Comparison of the size of the microstructure using DAS index for the 3 welding techniques

It appears that the dendrite arm spacing the smallest in the electron beam welds, which solidified thus the most rapidly. The hybrid laser/MIG welds solidified apparently less rapidly, because of larger dendrite arm spacing.

Finally, MIG dual wire welds show larger dendrite arm spacing than the welds of the other welding techniques. It can be concluded that the solidification of the

MIG welds was less rapid. And a greater quantity of dendrites has been observed in the MIG welds. These results are summarized numerically in the table 10 below:

Table 10 : Average DAS and local solidification time for the three welding techniques

WELDING TECHNIQUES	AVERAGE DENDRITE ARM SPACING (IN μM)	AVERAGE LOCAL SOLIDIFICATION TIME (IN SECONDS)
MIG dual wire	8.1	0.93
Electron beam	3.4	0.025
Hybrid Laser/MIG	4.7	0.13

Results of cell size measurements in equiaxed zone

Cell size measurements were performed exclusively in the case of electron beam welding. Such measurements are not applicable in the case of MIG welding.

The results are plotted in the Figure 44 below:

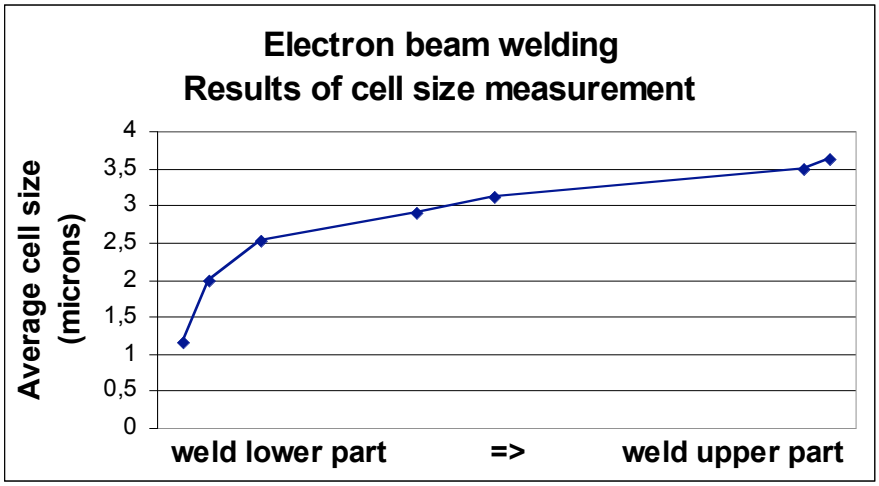

Figure 44: Electron beam – Results of cell size measurements

Cell size measurements along a vertical axis clearly show that the microstructure is much finer in the lower part of the weld, which thus solidified more rapidly.

Conclusion

It has been observed in the case of the MIG dual wire welding technique, for which the most dendrite arm spacings were measured, as well as in the case of the electron beam technique, that the local solidification time is lower in the part close to the cast than close to the sheet.

Even if nothing could be concluded in the case of the MIG welding process, it has been observed in the case of the electron beam welding technique that the size of the microstructure is much smaller at the bottom of the weld than at the top of the weld. The local solidification time will be thus lower at the bottom of the weld.

It can then be concluded that the weld has more rapidly solidified at the bottom of the weld and close to the cast than at the top of the weld and close to the sheet.

Micro-hardness results

MIG welding technique

The results of the micro-hardness evaluation of the MIG dual wire welds are represented on the transversal cut Figure 45 below:

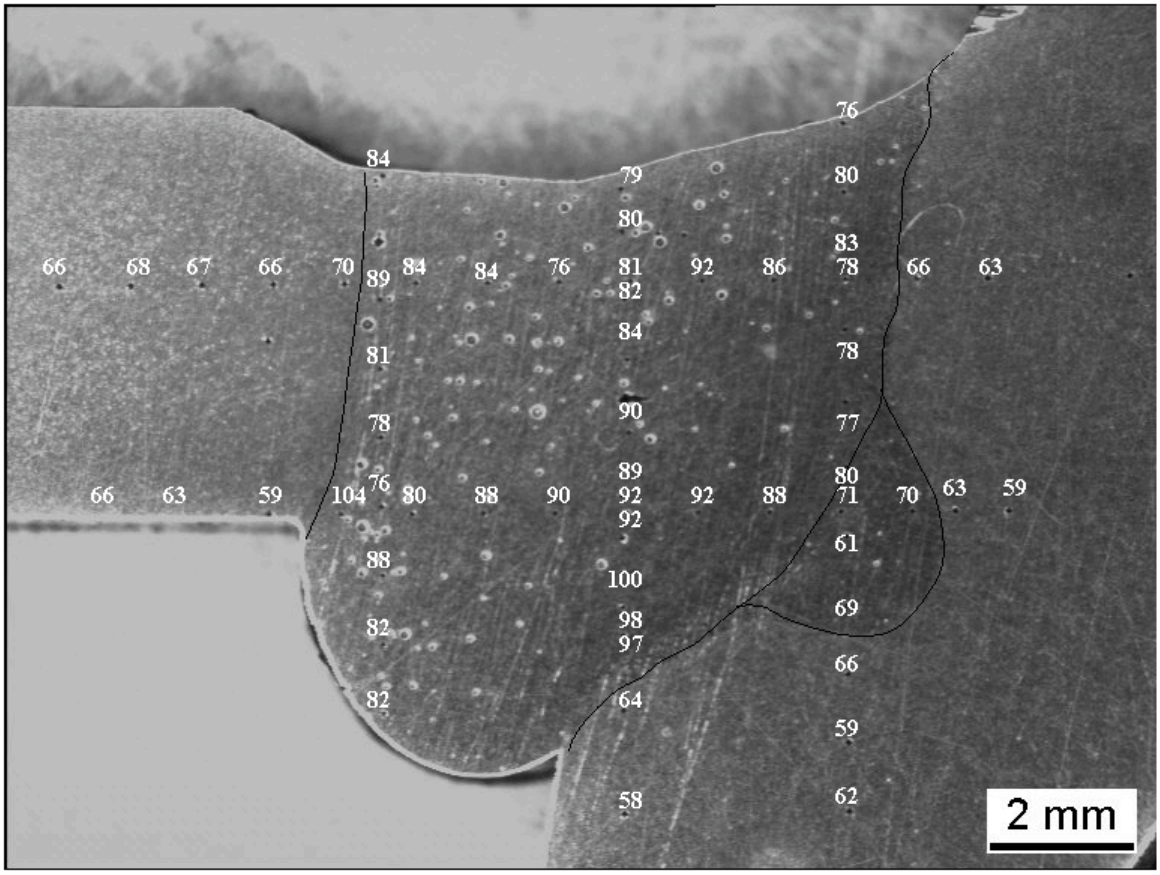

Figure 45: MIG micro-hardness results

The weld is harder than the sheet and the cast (average hardness is respectively 84 HV, 65 HV and 62 HV).

Hybrid laser/MIG welding technique

The results of the micro-hardness evaluation of the hybrid laser/MIG welds are represented on the transversal cut Figure 46 below:

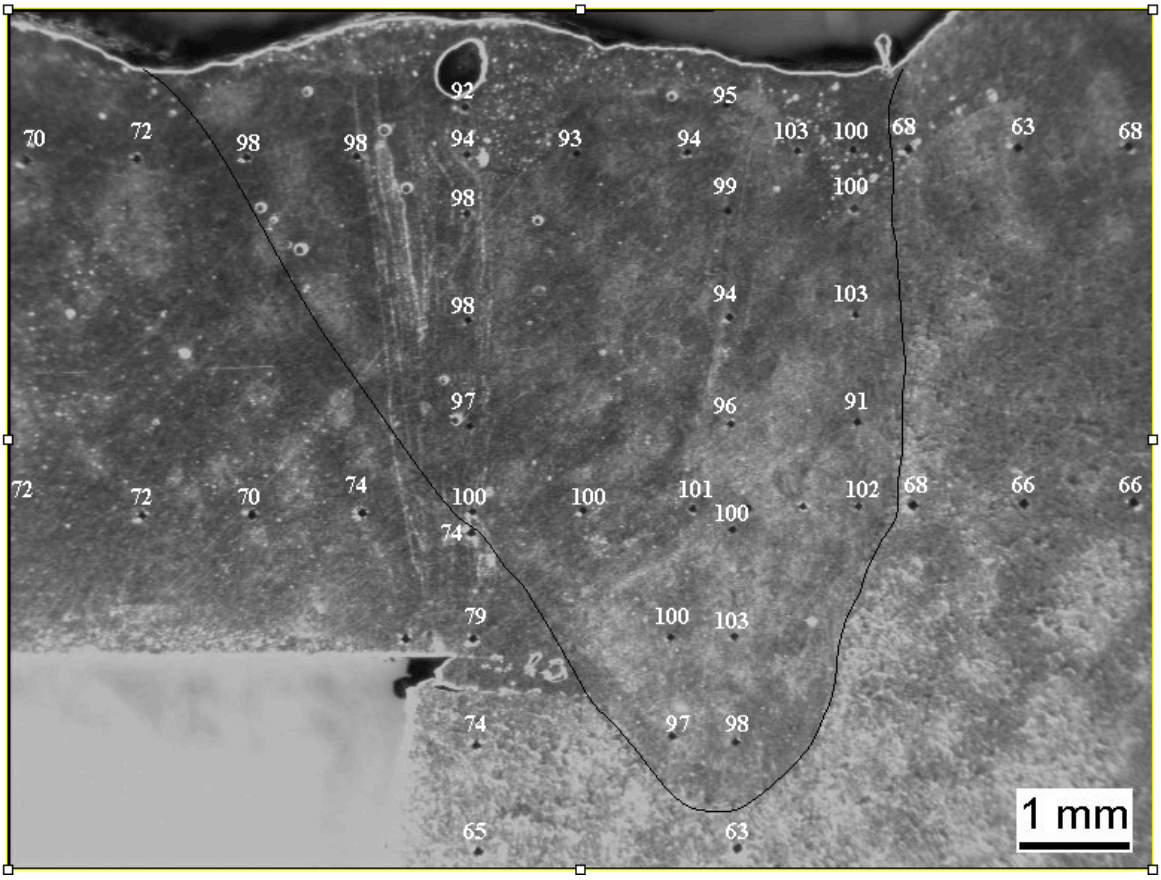

Figure 46: Laser Hybrid micro-hardness results

The weld is much harder than the sheet and the cast (average hardness is respectively 98 HV, 72 HV and 68 HV).

Electron beam welding technique

The results of the micro-hardness evaluation of the electron beam welds are represented on the transversal cut Figure 47 below:

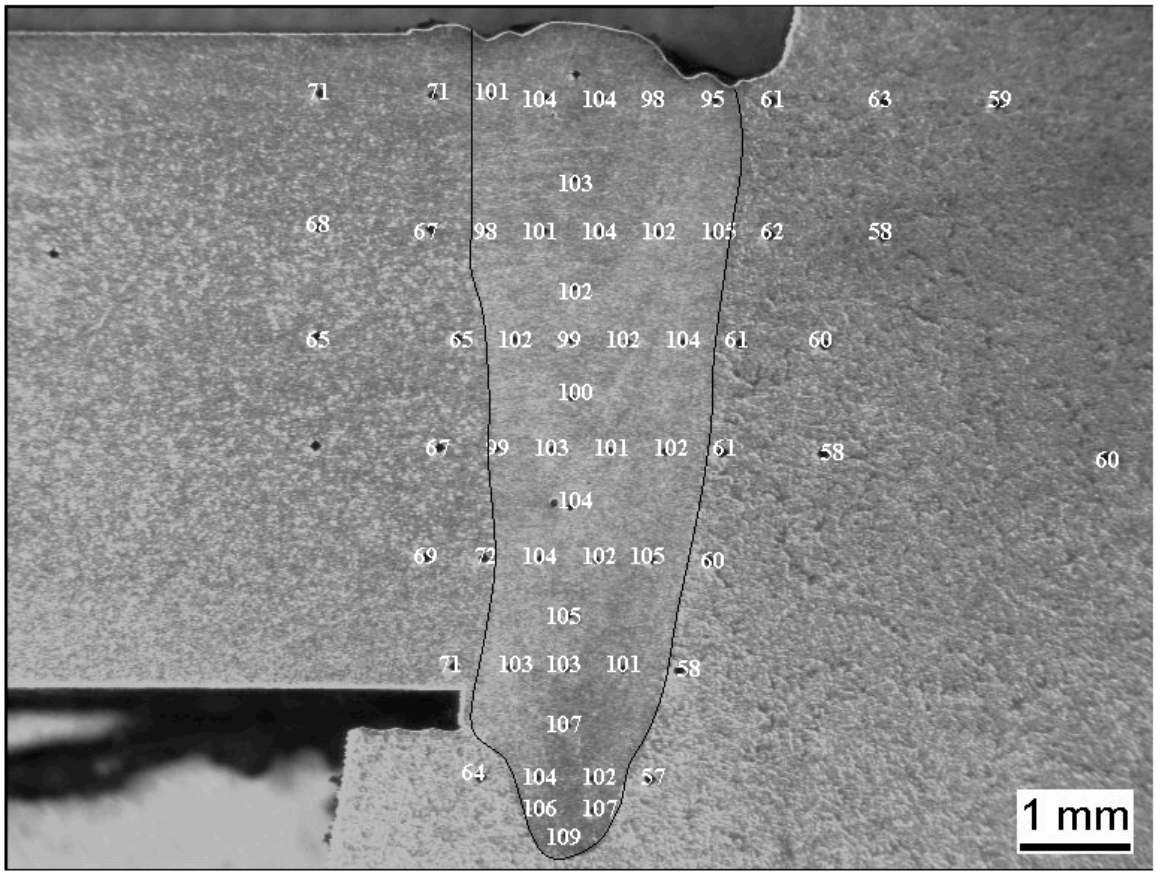

Figure 47: Electron beam micro-hardness results

The weld is in this case also much harder than the sheet and the cast (average hardness is respectively 102 HV, 68 HV and 60 HV).

Conclusions on micro-hardness results

For the three considered welding techniques, it appears that the sheet is a little bit harder than the cast, and that the welds are much harder than the sheet and the cast (see Table 11 below):

Table 11 : Results of micro-hardness analysis

	WELDING TECHNIQUE			
	MIG dual wire	Hybrid Laser/MIG	Electron beam	**Global average**
Average of measured hardness in the sheet (HV)	62	66	60	*63*

Average of measured hardness in the weld (HV)	84	98	102	*95*
Average of measured hardness in the cast (HV)	65	72	68	*68*

Inside the welds, globally, the part close to the cast and the bottom of the welds are harder than the part close to the sheet and the top of the weld.

According to Hall-Petch, finer is the microstructure greater is the hardness. Hall Petch law is verified in our case, and the harness results confirm the obtained microstructure results.

SEM results: Variation of chemical composition

MIG dual wire welding technique

On the Figure 48 below, the hardness results are compared to the EDX results (Si content) along a first horizontal axis:

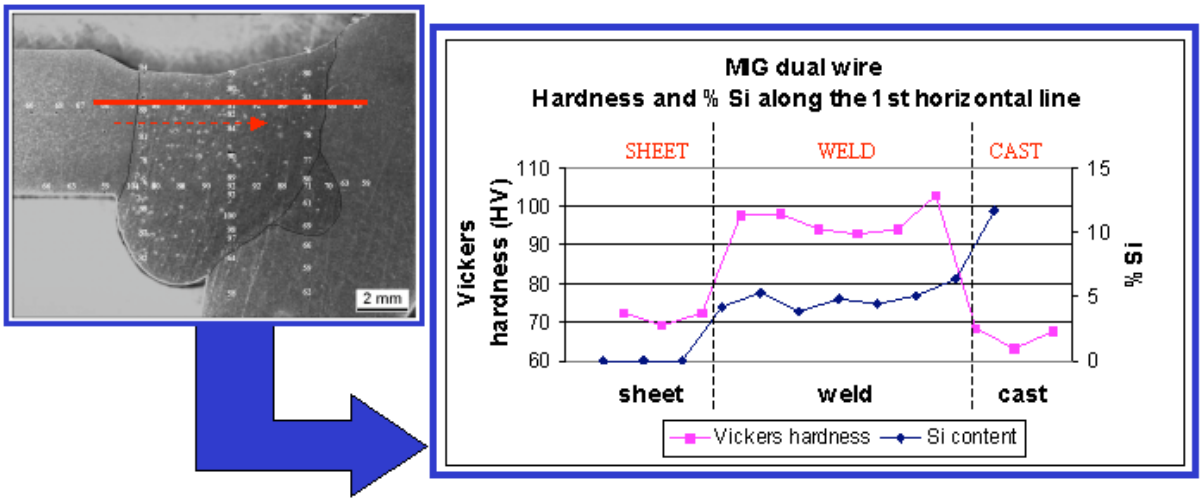

Figure 48: MIG – hardness versus Silicon content along a 1st horizontal axis

It should be noticed that the hardness is the greatest in the part close to the cast, lower in the part close to sheet, and the lowest hardness is measured at the

center of the weld. These results confirm the ones obtained through microstructure analysis by optical microscopy (see Figure 40 (a)).

The silicon content is quite homogeneous inside the weld.

On the Figure 49 below, the hardness results are compared to the EDX results (Si content) along a second horizontal axis:

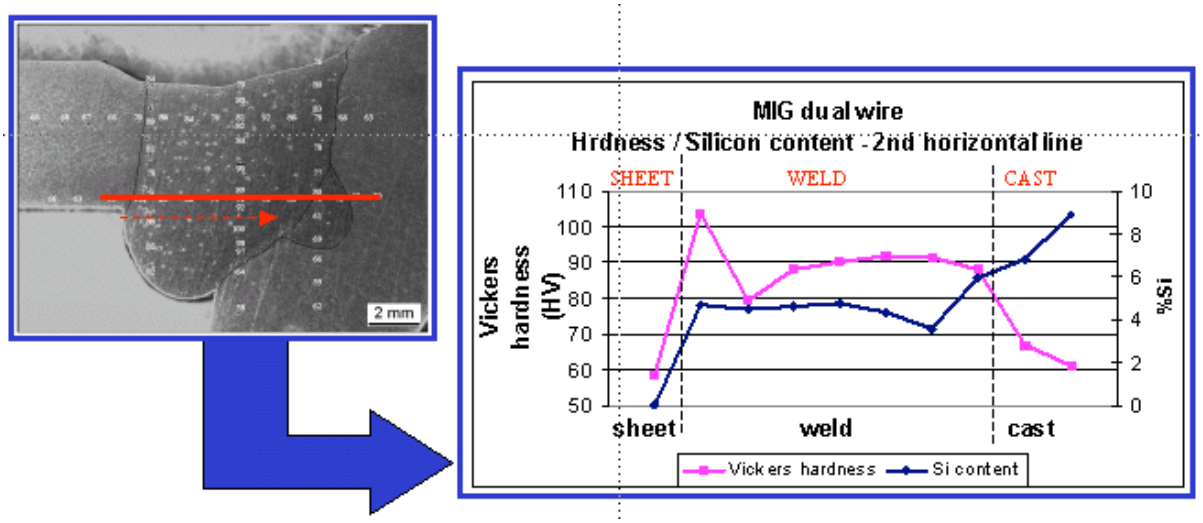

Figure 49: MIG – hardness versus Silicon content along a 2nd horizontal axis

Hybrid Laser/MIG welding technique

On the Figure 50 below, the hardness results are compared to the EDX results (Si content) along a horizontal axis:

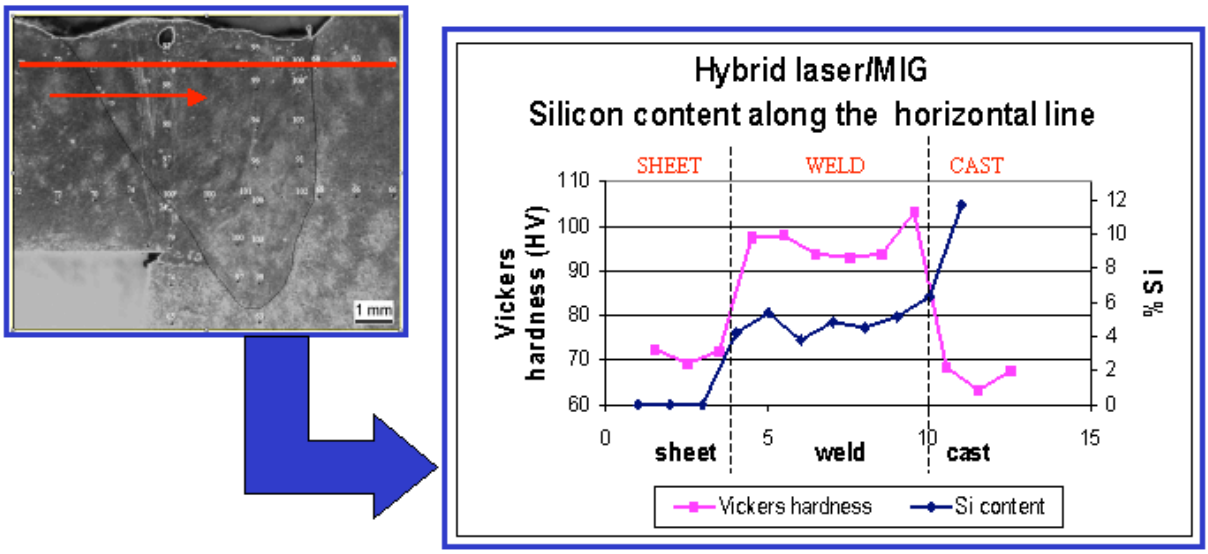

Figure 50: Hybrid Laser/MIG – hardness versus Silicon content along a horizontal axis

On the Figure 51 below, the hardness results are compared to the EDX results (Si content) along a vertical axis:

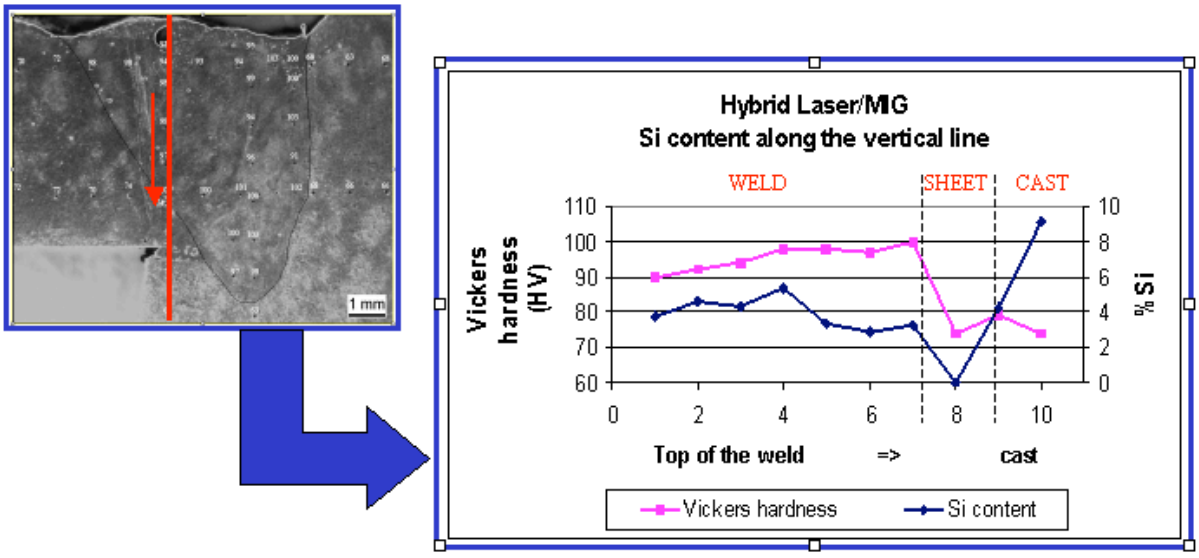

Figure 51: Hybrid Laser/MIG – hardness versus Silicon content along a vertical axis

Electron beam welding technique

On the Figure 52 below, the hardness results are compared to the EDX results (Si and Mg content) along a defined horizontal axis:

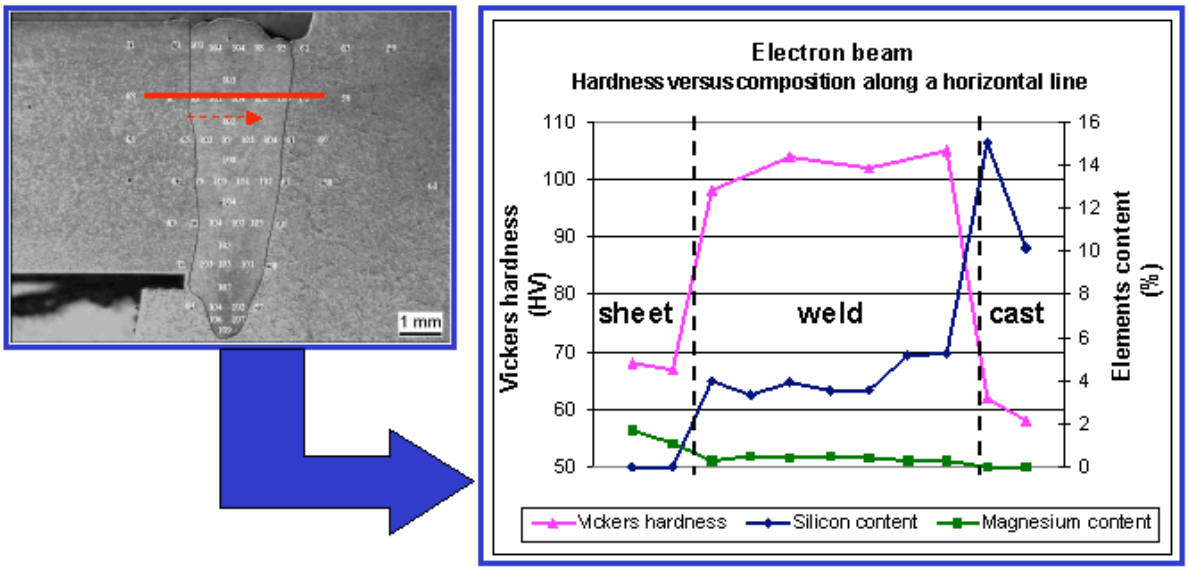

Figure 52: Electron beam – hardness versus Silicon content and Magnesium content along a horizontal axis

On the Figure 53 below, the hardness results are compared to the EDX results (Si and Mg content) along a vertical axis:

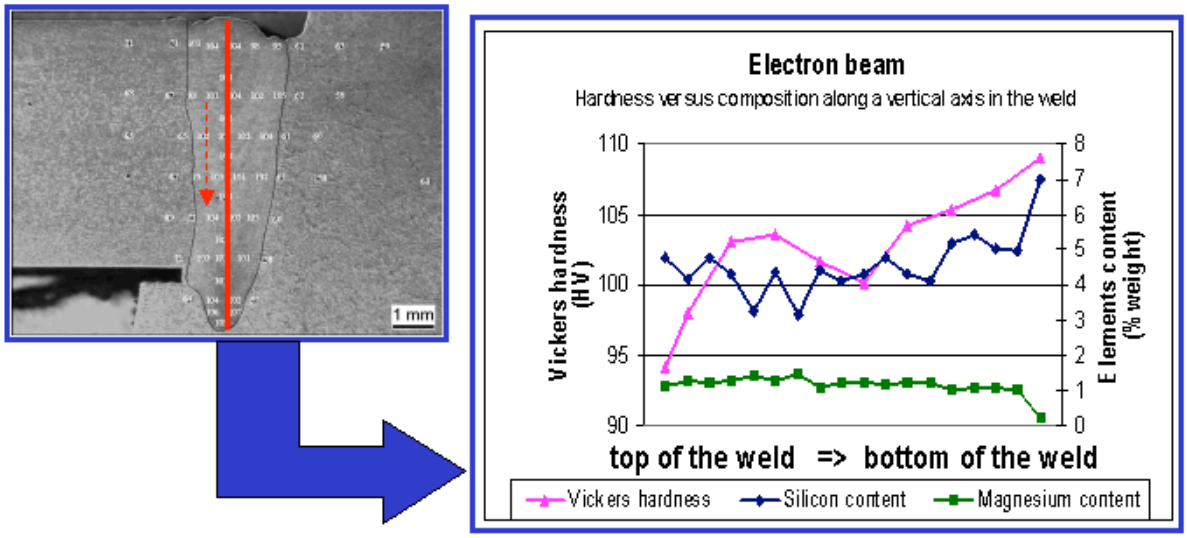

Figure 53: Electron beam – hardness versus Silicon content and Magnesium content along a vertical axis

The hardness globally increases from the top of the weld to the bottom of the weld. This confirms the results of microstructure analysis by cell size measurement (see Figure 44).

The silicon content is greater in the pocket at the bottom of the weld, probably due to the proximity to the cast.

Conclusions on the electron microprobe analysis

The different values of Silicon content along the lines let us distinguish the different characteristic zones (sheet/weld/cast).

Inside the weld, the silicon content presents a small variation. The average of Silicon content is 4.5% (see Figure 54).

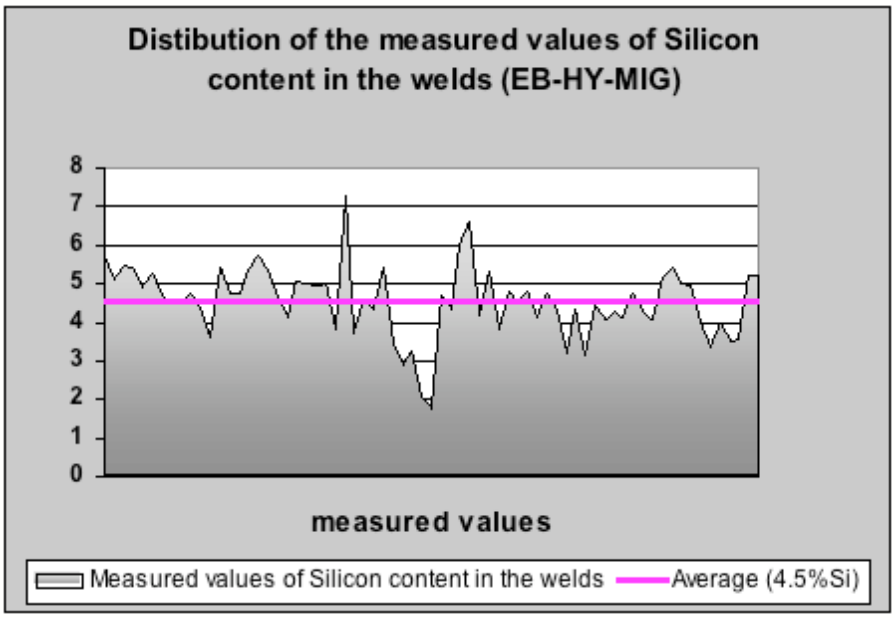

Figure 54: Distribution of the silicon content measurements inside the weld

It appears that the silicon content has been homogenized in the weld bead due to the convection effect inside the molten metal.

The average values of composition inside the welds of each welding technique are represented in the Table 12 below:

Table 12: Average composition values inside the weld

Welding technique	Silicon content (Weight %)	Magnesium content (Weight %)
MIG dual wire	5.0	0.7
Electron beam	4.2	1.2
Hybrid Laser/MIG	4.3	1.3

The average magnesium content in the sheet is 2.9 wt%. According to the EDX results, there has been an important magnesium loss in the case of the MIG process.

According to Damien Fabregue [2], the hardness increases with the silicon content. Because in one hand we can read on the Al-Si phase diagram that the eutectic point corresponds to 12% Si, and in the other the homogenized molten bead presents 4.5% Si, there should be segregation of silicon inside the weld.
Unfortunately, this segregation was not detected through this EDX analysis. And Fabregue's conclusion was not verified in our case, because hardness depends also on the size of the microstructure, which is inhomogeneous in the analyzed welds.
This point needs to be confirmed by further experimental investigation.

Proposal of porosity formation mechanisms

Porosity formation could be partly due to the selective boiling of Magnesium present in the sheet. The MIG dual wire welds presents the coarser microstructure, the lowest hardness; we could thus believe that they solidified the less rapidly. The MIG welds also show almost two times less magnesium.

This mechanism could be a cause of porosity formation, but this point needs to be confirmed by further electron microprobe analysis on porosity walls, by measuring the magnesium content in the pores especially for MIG dual wire welds.

MIG welding technique

Only micropores having a diameter lower than below 280 microns were present in the MIG welds.

Knowledge related to the materials properties/geometries

It is known that:

- The heat escapes through the weld/metal interface rather than through the weld/air interface
- The cast has a greater heat capacity than the sheet, and allows a greater heat flux
- The contact surface with the cast is greater than with the sheet

For these reasons, more heat will escape through the weld/cast interface.

Therefore, the velocity of the Solid/Liquid interface will be greater in the zone close to the cast, rather than the one close to the sheet and than the one close to the air

Results on porosity distribution analysis

It has been shown in the previously that greater amounts of porosity are located in the part close to the sheet, and in the upper part of the weld.

Conclusion

The mechanism of hydrogen segregation is proposed to explain the formation and the distribution of the porosity in the MIG welds.

Hybrid Laser/MIG welding technique

Paper review

Concerning the YAG laser welding technique of on one hand a wrought alloy AA5083-O with a high Mg content (4.5%) and on the other hand an A356 cast alloy (7% Si), Haboudou et al. [4] showed in 2003, generates two kind of two kind of porosity.

The first one is microporosity, which are mostly ascribed to hydrogen solubility in aluminum.

The second kind of porosity may be called macrocavities, having a diameter greater than 300 microns. Their shape is less circular than hydrogen occluded pores. These pores are not attributed to hydrogen rejection. They are mostly due to keyhole closure or shrinking and process instability. These cavities are much circular than microporosity and have certainly been initiated at the keyhole root, which is a common occurrence during laser welding in keyhole mode. They are localized mostly at the edges and at the root of the bead.

Microporosity

It has been shown previously that most of the microporosity is located in the part close to the sheet, and in the upper part of the weld.

For the same reasons as for the MIG dual wire welding technique, the mechanism of hydrogen segregation is proposed to explain the formation and the distribution of the porosity in the hybrid laser/MIG welds.

Macroporosity

It has been shown in this paper that most of the macroporosity is located at the bottom of the weld, or close to the edges of the weld.

According to Haboudou et al., the instability of the keyhole leading to shielding gas entrapment could be the main mechanism involved in the formation of macroporosity or macrocavities.

Electron beam welding technique

Because of the negligible amount of porosity present in the electron beam welds, a mechanism of porosity formation is difficult to propose.

Nevertheless, in the case of electron beam welding, we should keep in mind that fujii et al [5] showed in 2004 that the pores are formed through a reaction between the molten aluminum and aluminum oxide present at the surface, forming Al2O gas. These gas bubbles could then grow by hydrogen diffusion and coalescence with each other.

In our case, micro-hardness analysis showed that the hardest part of the weld is the bottom. This result is confirmed by the DAS measurements, showing that the bottom of the weld presents a very fine microstructure; it is thus believed that the bottom of the weld has very rapidly solidified, leading to gas entrapment and spike formation.

SUMMARY AND CONCLUSIONS

Radiography and optical microscopy results have shown that, knowing that different welding parameters have been used and different surface preparations have been carried out before welding, electron beam welding technique has provided the best results in terms of low porosity formation, followed by the MIG dual wire welding technique. A greater amount of porosity, caused by the presence of many macrocavities, has been observed in the hybrid laser/MIG welds.

The 3 different types of welds mentioned above have presented a different solidification speed, but similar directions of solidification and similar relative solidification velocities. Indeed, it has appeared that the weld/metal interfaces solidified the most rapidly, the weld/cast interface showing the lowest solidification time. Thus, solidification time within weld was the greatest in a upper part, which is closer to the sheet than to the cast. In addition, the hybrid laser MIG and the electron beam welds have solidified the most rapidly, the electron beam welds presenting the lowest solidification time, as well as the greatest hardness.

Mechanisms of porosity formation have been proposed for the welding techniques under evaluation; in one hand, microporosity distribution analysis seems to show that its formation is mainly due to hydrogen, whose presence in the molten metal leads to nucleation and growth of porosity during solidification; in an other hand the literature suggests that macroporosity formation comes from the instability of the keyhole.

Nevertheless, the contribution of other porosity formation mechanisms is not excluded; gas formation by chemical reaction, or evaporation of low boiling points elements such as magnesium could play a non-negligible role in the formation of porosity.

The influence of this last mentioned mechanism needs to be further evaluated by electron microprobe analysis inside the pores. It would also be interesting to analyze the chemical composition inside the pores after solidification.

As a next step, it appears to be interesting to select a welding technique and carry out a parametric study, aiming to optimize the welding parameters in order to reduce the level of porosity inside the welds. The results of the parametric study will give tools helping to carry out a modeling work.

REFERENCES

[1] ASM Specialty handbook, “Aluminum and aluminum alloys”, 1993.

[2] Damien Fabregue, “Microstructure et fissuration à chaud lors du soudage laser d’alliages d’aluminium 6000”, thèse, 2004.

[3] P.D. Lee, P.N. Quested, M. McLean, “Modelling of Marangoni effects in electron beam melting”, Philosophical Transactions: Mathematical, Physical and Engineering Sciences, Vol 356, pp 1027-1043, 1998.

[4] A.Haboudou, P.Peyre, A.B Vannes, G.Peix, “Reduction of porosity content generated during Nd:YAG laser welding of A356 and AA5083 aluminum alloys”, Materials science and engineering, A363, pp 40-52, 2003.

[5] Hidetoshi Fujii, Kiyoshi Nogi, Yasuhiro Aoki, Hideaki Umatoshi, “Bubble formation in aluminum alloy during electron beam welding”, Journal of Materials Processing Technology 155-156, pp 1252-1255, 2004.